HHS Public Access

Author manuscript

Dev Dyn. Author manuscript; available in PMC 2019 August 01.

Published in final edited form as:

Dev Dyn. 2018 August ; 247(8): 976–991. doi:10.1002/dvdy.24639.

Alterations in Retinoic Acid Signaling Affect the Development of the Mouse Coronary Vasculature

Suya Wang[a], **Weiliang Huang**[b], **Hozana A. Castillo**[c], **Maureen A. Kane**[b], **José Xavier-Neto**[d], **Paul A. Trainor**[e,f], and **Alexander R. Moise**[a,g,1]

[a]Department of Pharmacology and Toxicology, School of Pharmacy, University of Kansas, Lawrence, KS, 66045, USA

[b]Department of Pharmaceutical Sciences, School of Pharmacy, University of Maryland, Baltimore, MD, 21201, USA

[c]Brazilian Biosciences National Laboratory, LNBio, Rua Giuseppe Máximo Scolfaro, 10.000, Polo II de Alta Tecnologia de Campinas, Campinas, SP, Brazil

[d]Conselho Nacional do Desenvolvimnto Científico e Tecnológico (Cnpq) CEP 01414000 Cerqueira Cesar Sao Paulo, Sao Paulo, Brazil

[e]Stowers Institute for Medical Research, Kansas City, MO, 64110, USA

[f]Department of Anatomy and Cell Biology, University of Kansas Medical Center, Kansas City, KS, 66160, USA

[g]Northern Ontario School of Medicine, Biomolecular Sciences Program and Department of Chemistry and Biochemistry, Laurentian University, Sudbury, ON, P3E 2C6, Canada

Abstract

Background—During the final stages of heart development the myocardium grows and becomes vascularized via paracrine factors and cell progenitors derived from the epicardium. There is evidence to suggest that retinoic acid (RA), a metabolite of vitamin A, plays an important role in epicardial-based developmental programming. However, the consequences of altered RA-signaling in coronary development have not been systematically investigated.

Results—We explored the developmental consequences of altered RA-signaling in late cardiogenic events that involve the epicardium. For this, we employed a model of embryonic RA excess based on mouse embryos deficient in the retinaldehyde reductase DHRS3, and a complementary model of embryonic RA deficiency based on pharmacological inhibition of RA synthesis. We found that alterations in embryonic RA-signaling led to a thin myocardium and aberrant coronary vessel formation and remodeling. Both excess, and deficient RA-signaling are associated with reductions in ventricular coverage and density of coronary vessels, altered vessel morphology and impaired recruitment of epicardial-derived mural cells. Using a combined transcriptome and proteome profiling approach, we found that RA treatment of epicardial cells influenced key signaling pathways relevant for cardiac development.

[1]To whom correspondence should be addressed: Alexander Moise, Ph.D.; Medical Sciences Division, Northern Ontario School of Medicine, 935 Ramsey Lake Rd., Sudbury, ON, P3E 2C6, Canada. Phone: 705-662-7253. amoise@nosm.ca.

Conclusions—Epicardial RA-signaling plays critical roles in the development of the coronary vasculature needed to support myocardial growth.

Keywords

Congenital heart defect; Coronary Vascular Development; Epicardium; Heart development; Myocardial Growth; Retinoic Acid; Vitamin A

INTRODUCTION

Retinoic acid (RA), an active metabolite of vitamin A, carries out regulatory roles in many essential processes during both embryonic and postembryonic life (Clagett-Dame and Knutson, 2011). The activities of RA are mediated by ligand-activated transcription factors, known as retinoic acid receptors (RARs) and retinoid X receptors (RXRs), which are found associated with DNA motifs, termed RA response elements (RAREs), in the vicinity of target genes (Cunningham and Duester, 2015). Binding of RA to RAR/RXR heterodimers leads to the activation, or repression, of hundreds of genes resulting in pleiotropic effects, which influence tissue growth, differentiation and repair (Paschaki et al., 2013). RA-signaling is regulated by a complex transport and enzymatic pathway, which controls the levels of available cellular RA (reviewed in (Shannon et al., 2017)). The cellular RA levels are also influenced by the health and nutritional status of the individual, which can affect, the dietary availability, uptake, or tissue storage of retinol and provitamin A carotenoid precursors (Rubin et al., 2017).

Alterations in RA-signaling resulting from excess or deficiency of dietary vitamin A, or due to treatment with RAR agonists can lead to congenital disorders manifested as craniofacial, cardiac, limb, thymus, ear and neural tube malformations (Kochhar, 1973; Lammer et al., 1985; Rothman et al., 1995; Vieux-Rochas et al., 2007; Ackermans et al., 2011). The magnitude of the teratogenic effects of altered RA-signaling depends both on the extent of deficiency or excess, and on the developmental stage of the fetus at the time of exposure (Collins and Mao, 1999). The development of the heart is very sensitive to altered RA levels. Better understood are the effects of RA on early stages of cardiogenesis, when RA controls the determination of the cardiogenic progenitor pool and the anteroposterior patterning of the primitive heart tube (reviewed in (Xavier-Neto et al., 2015; Stefanovic and Zaffran, 2017). As a result, altered RA-signaling can induce a series of defects related to looping, outflow tract and chamber formation (Lammer et al., 1985; Lee et al., 1997; Yasui et al., 1997; Kolodzinska et al., 2013). Paradoxically, excess and deficiency of RA can often result in similar defects, due to either compensatory mechanisms or simply because both excess or deficiency of RA ultimately result in impaired development (Frenz et al., 2010; Lee et al., 2012; Rydeen et al., 2015)

Following the formation of the chambered heart, RA-signaling is involved in several late developmental processes in the embryonic heart, which include the growth of the myocardial compact zone and the formation of the coronary vasculature. The main source of RA in the late heart is the epicardium, a mesothelial layer of cells that covers the heart starting at E9.5–E10 in mouse embryos (Moss et al., 1998). The epicardium secretes trophic factors, which

support myocardial expansion, such as Fibroblast Growth Factor (FGF) 2 and 9 the latter of which is responsive to intrinsic epicardial RA signaling (Lavine et al., 2005). The epicardium also responds to extra-cardiac RA signaling. For example, embryonic liver RA signaling stimulates erythropoietin (EPO) secretion to induce the production of insulin-like growth factor 2 (IGF2) in the epicardium, which stimulates myocardial expansion (Brade et al., 2011; Shen et al., 2015). Thereby, an RA-Epo-Igf2 signaling axis operating from the fetal liver to the epicardium coordinates erythropoiesis with myocardial growth. Moreover, epicardial-derived precursor cells (EPDCs) undergo epithelial-to-mesenchymal transition (EMT) giving rise to cardiac vascular smooth muscle cells (VSMCs) and perivascular and interstitial fibroblasts, which stabilize the coronary vasculature and provide functionality to the contracting heart (reviewed in (Lajiness and Conway, 2014; Sharma et al., 2017). Since, the formation of the vasculature and myocardial compaction must proceed in a timely and well-orchestrated manner, defects in the formation of epicardial derivatives are often associated with both compromised formation of coronary vessels and hypoplastic ventricles (Smith et al., 2011; von Gise et al., 2011; Trembley et al., 2015; Singh et al., 2016). This is also true in the case of mouse models of altered RA-signaling, which manifest both thin myocardium (Chen et al., 2002; Stuckmann et al., 2003; Brade et al., 2011; Shen et al., 2015) as well as defects in the formation of the coronary vasculature (Merki et al., 2005; Lin et al., 2010). However, despite the evidence of the contribution of RA-signaling in late heart development, many questions remain regarding its exact roles in this process.

Here, we examined the effects of altered RA-signaling during late gestation development of the heart focusing on coronary vessel formation and myocardial growth. Recent studies suggest that RA may play an important role in the epicardial cytoskeletal rearrangement, migration and differentiation of EPDCs (Merki et al., 2005; Azambuja et al., 2010; Braitsch et al., 2012; Wang et al., 2018; Xiao et al., 2018). Using complementary models of either excess or deficiency of RA, we demonstrate that RA plays an indispensable role in the development of the primary endothelial plexus of the coronary vasculature and the recruitment of mural cells by the endothelial bed. In addition, both excess and deficiency of RA were found to cause reduction in the ventricular myocardial growth. Through a combined transcriptome/proteome analysis, we found that *in vitro* activation of RA-signaling in epicardial cells led to changes in expression of genes involved in cardiogenic pathways such as FGF, Serum Response Factor (SRF) and Hypoxia-Inducible Factor 1-α (HIF1-α). Taken together, our study describes the effects of altered RA-signaling on the development of the coronary vasculature and the myocardium and provides evidence for the requirement of epicardial RA signaling to orchestrate the development of the coronary vasculature required to support myocardial expansion.

RESULTS

Excess RA affects development of the heart during late gestation

To test the teratogenic effect of excess RA on development of the heart, we employed a mouse model lacking the enzyme, DHRS3, which reduces the RA precursor, retinaldehyde, to retinol and thus prevents the synthesis of excess RA (Haeseleer et al., 1998). Studies from our lab and others have previously shown that in the absence of *Dhrs3*, RA accumulates and

causes alterations in RA-signaling both globally and within the developing hearts of *Dhrs3*$^{-/-}$ embryos (Feng et al., 2010; Billings et al., 2013; Kam et al., 2013; Adams et al., 2014; Wang et al., 2018). Here, we first asked whether *Dhrs3*-ablation results in altered RA-signaling in the hearts of *Dhrs3*$^{-/-}$ mice at E12.5, a stage marked by the rapid myocardial growth and coronary plexus development. We crossed the *Dhrs3*$^{+/-}$ mice with the *RARE-LacZ* mouse strain, which expresses a *LacZ* reporter gene driven by a promoter controlled by a RARE derived from the mouse *Rarb* promoter (Rossant et al., 1991). This allowed us to visualize the tissues exhibiting active RA-signaling in the developing embryos. The detection of *LacZ*-encoded β-galactosidase revealed that at E12.5, ablation of *Dhrs3* causes an expansion of RA-signaling in the mutant heart (not shown), which agrees with findings of *RARE-LacZ* gene expression observed in E10.5 and E14.5 *Dhrs3*$^{-/-}$ embryos (Billings et al., 2013; Shannon et al., 2017; Wang et al., 2018). The expansion of RA-signaling seen in the hearts of *Dhrs3*$^{-/-}$ embryos is also consistent with the observed increases in the global levels of RA as quantified by direct analysis via LC-MS/MS at E12.5 and E14.5 in *Dhrs3*$^{-/-}$ embryos (Billings et al., 2013; Wang et al., 2018).

When *Dhrs3*$^{+/-}$ dams were fed on a vitamin A sufficient (VAS) diet containing 4 IU preformed vitamin A per gram of food, their *Dhrs3*-null offspring (VAS-*Dhrs3*$^{-/-}$) displayed mid-gestational lethality accompanied by defects in the development of the heart. As we have previously reported, global ablation of *Dhrs3* is associated with a membranous ventricular septal defect, agenesis of the atrial septum and a double-outlet right ventricle (DORV) in E14.5 VAS-*Dhrs3*$^{-/-}$ embryos (Billings et al., 2013). Examination of the gross morphology of the E14.5 VAS-*Dhrs3*$^{-/-}$ embryos presented evidence of peripheral edema suggesting cardiac insufficiency in the absence of *Dhrs3* (Fig. 1A *vs.* B). The ventricular myocardium of E14.5 VAS-*Dhrs3*$^{-/-}$ embryos exhibited a 2-fold reduction in the thickness of its compact zone in comparison to wild type littermates (VAS-wild type) (Fig 1C *vs.* D, via hematoxylin and eosin quantified in 1E). This phenotype is similar to observations made in other models with altered RA-signaling (Niederreither et al., 2001; Merki et al., 2005; Lin et al., 2010).

Ablation of *Dhrs3* is also associated with defects and delays in the formation of the coronary vasculature. Most notably, on the ventral side of the ventricles of E14.5 VAS-*Dhrs3*$^{-/-}$ embryos, we observed larger numbers of PECAM1-positive endothelial nodules of greater size and broader distribution than seen in their VAS-wild type littermates (Fig 2A *vs.* B, quantified in 2D). Such epicardial PECAM1-positive nodules may originate as ectopic blood islands and have been observed in other mouse models that exhibit defects in the development of the coronary vasculature (Mellgren et al., 2008; Tian et al., 2013; Wu et al., 2013; Trembley et al., 2015). Additional related cardiovascular defects became noticeable VAS-*Dhrs3*$^{-/-}$ hearts at E14.5. As the primitive plexus matures, the vessels of the hearts of VAS-wild type littermates undergo remodeling, including pruning and branching (Fig. 2F). However, in the hearts of E14.5 VAS-*Dhrs3*$^{-/-}$ embryos, the vessels remained tortuous, aberrantly enlarged, and lacking branching from pre-existing vascular beds (Fig. 2G). This defect is especially noticeable near the atrioventricular canal (AVC) of the hearts of E14.5 VAS-*Dhrs3*$^{-/-}$ embryos, where the vessels formed a large endothelial mass, with few branches (Fig 2G, red arrow). In addition, the hearts of E14.5 VAS-*Dhrs3*$^{-/-}$ embryos displayed reduced coronary vessel coverage of the heart compared to VAS-wild type

littermates (Fig. 2F *vs.* G). Therefore, excess embryonic RA and expanded RA-signaling observed in the hearts of VAS-*Dhrs3*$^{-/-}$ embryos is associated with coronary defects.

To confirm that the coronary vessel malformations observed in *Dhrs3*$^{-/-}$ embryos develop as a consequence of excessive RA, we fed *Dhrs3*$^{+/-}$ dams from weaning with a vitamin A-deficient (VAD) diet to generate VAD-*Dhrs3*$^{-/-}$ embryos. Our hypothesis was that the lower levels of RA precursors found in VAD-*Dhrs3*$^{-/-}$ embryos would reduce the levels of RA being formed and restore normal development in *Dhrs3*$^{-/-}$ embryos. Indeed, feeding *Dhrs3*$^{+/-}$dams a VAD diet led to restoration of vascular coverage of the dorsal ventricles of VAD-*Dhrs3*$^{-/-}$ embryos to the levels observed in E14.5 VAS-wild type littermates (Fig. 2H *vs.* G and *vs.* F, quantified in 2E). Moreover, feeding *Dhrs3*$^{+/-}$ dams a VAD diet also led to reduced formation of endothelial nodules in the *Dhrs3*$^{-/-}$ hearts (Fig 2C *vs.* B) compared to hearts of VAS-*Dhrs3*$^{-/-}$ embryos. In fact, feeding dams a VAD diet for three successive generations, allowed us to bypass the embryonic lethality associated with the *Dhrs3*-deficiency to obtain viable *Dhrs3*$^{-/-}$ pups that survived into adulthood (Supplement Movie 1). In conclusion, our data suggest that the cardiac developmental defects resulting from genetic deletion of *Dhrs3* are chiefly caused by increased formation of RA.

Coronary vessels of E14.5 VAS-*Dhrs3*$^{-/-}$ hearts had an altered morphology. Whereas wild type hearts developed extensive arborization including both small and large vessels, coronary vessels of VAS-*Dhrs3*$^{-/-}$ hearts were consistently larger (PECAM1 immunostaining Fig. 2K *vs.* L, quantified in 2I). In addition, VAS-*Dhrs3*$^{-/-}$ hearts had significantly reduced vascular density per area of myocardium (Fig. 2J). In particular, there was an accumulation of dilated and superficial vessels in the subepicardial space of VAS-*Dhrs3*$^{-/-}$ embryos (Fig. 2L, white arrowheads), which we identified as COUP-TFII-positive veins (Fig 2M *vs.* N). However, *in situ* hybridization of COUP-TFII in VAS-*Dhrs3*$^{-/-}$ hearts at E9.5 revealed relatively normal localization and expression levels of COUP-TFII in the primitive VAS-*Dhrs3*$^{-/-}$ heart tube, suggesting that the expression of COUP-TFII at early stages as well as the patterning of the primitive heart tube was normal (not shown). Thus, altered RA homeostasis led to perturbations in the morphology, organization and vascular density of coronary vessels in VAS-*Dhrs3*$^{-/-}$ mouse embryos. Taken together, our results suggest that excessive formation of RA in VAS-*Dhrs3*$^{-/-}$ embryos affects not only the cytoskeletal reorganization of epicardial cells and migration of epicardial cells reported previously (Wang et al., 2018), but also the subsequent development of their coronary vessels.

Excess RA does not affect vessel formation in the placenta and the embryonic yolk sac

RA was proposed to play a role in the development of the placental and yolk sac vascular plexuses (Lai et al., 2003) and in the formation of hematopoietic stem cells from the hemogenic endothelium (Chanda et al., 2013). Since deletion of *Dhrs3* has been found to cause global changes in alter RA-signaling, we assessed whether development of the placental, and yolk sac vascular plexuses was affected in *Dhrs3*$^{-/-}$ embryos. Histology analysis using hematoxylin and eosin revealed a normal placental morphology in VAS-*Dhrs3*$^{-/-}$ mice when compared with wild type littermates at E13.5 and E14.5 (Fig. 3A–D). Quantification of the thickness and density of the vascular labyrinth did not reveal any

significant differences between wild type and *Dhrs3* mutant embryos (Fig. 3E–F). Deletion of *Dhrs3* did not impede the formation and branching of vascular tubes from the chorionic plate, nor did it impact placental vascular patterning (Fig. 3G–J). In addition, both VAS-*Dhrs3*$^{-/-}$ embryos and their stage-matched wild type littermates had an intact embryonic yolk sac plexus composed of a finely branched and properly developed network as illustrated by whole-mount PECAM1 immunostaining (Fig. 3K, L). Therefore, altered RA-signaling in VAS-*Dhrs3*$^{-/-}$ embryos did not affect vasculogenesis and remodeling of placental and yolk sac plexuses.

Excess RA interferes with the recruitment and differentiation of VSMC progenitors

VSMCs and pericytes are critical for coronary vessel morphogenesis and function (Mellgren et al., 2008; Trembley et al., 2015). Coronary vascular mural cells, which are derived predominantly from the epicardium via an EMT, migrate into the myocardium where they are required in vascular stabilization and remodeling (Smith et al., 2011). We and others have shown that RA-signaling plays a critical role in both the formation, migration and differentiation of epicardial cells (Azambuja et al., 2010; Braitsch et al., 2012; Wang et al., 2018). Specifically, *Dhrs3*$^{-/-}$ EPDCs were found to migrate deeper into the myocardium of E14.5 *Dhrs3*$^{-/-}$ mice (Wang et al., 2018; Xiao et al., 2018). Since studies described herein suggest that *Dhrs3*$^{-/-}$ mice have compromised coronary vasculature, we investigated if the recruitment of VSMCs by the coronary plexus is affected in *Dhrs3*$^{-/-}$ hearts.

We characterized the localization and recruitment of VSMC progenitors to the endothelial tubes by immunostaining with VSMC and endothelial markers, PDGFRB and PECAM1 respectively, in *Dhrs3*$^{-/-}$ and control hearts. PDGFRB marks not only progenitors of VSMCs but also pericytes that are recruited to capillaries and postcapillary venules. Most PECAM1-positive vessels were associated with PDGFRB-positive vessels at E14.5 in both wild type and *Dhrs3*$^{-/-}$ hearts (Fig. 4A–H, red arrows). However, we observed noticeably more PECAM1-positive endothelial tubes that were not associated with PDGFRB-positive VSMC progenitors in the *Dhrs3*$^{-/-}$ myocardium compared to wild type (Fig. 4C *vs.* G, yellow arrow). At the same time, there were more PDGFRB-positive cells unassociated with any vessels in the *Dhrs3*$^{-/-}$ hearts (Fig. 4C *vs.* G, white arrowheads).

The enlarged coronary vessels persisted in the few surviving E17.5 VAS-*Dhrs3*$^{-/-}$ fetuses, which exhibited a combination of normal-sized intramyocardial arteries and very large, collapsed, superficial veins compared to wild type controls (Fig. 5A *vs.* B, white arrows). When we examined the recruitment of VSMC progenitors in *Dhrs3*$^{-/-}$ embryos that survived to E17.5, we noticed a remarkable reduction in the number of PDGFRB-positive VSMC progenitors near PECAM1-positive vessels in the *Dhrs3*$^{-/-}$ hearts (Fig. 4I–P). This recruitment defect was most noticeable in the case of the large subepicardial veins observed in *Dhrs3*$^{-/-}$ hearts at E17.5 which were found to be devoid of mural PDGFRB-positive cells (Fig. 4K–L *vs.* 4O–P). Furthermore, VSMC progenitors failed to differentiate into mature VSMCs in *Dhrs3*$^{-/-}$ hearts when compared to wild type hearts, as revealed by the lack of expression of SM22α in mural cells around major vessels (Fig. 5C–H, yellow arrows). In contrast to larger vessels, PDGFRB-positive VSMCs or pericytes were found to be in direct contact with the PECAM1-positive endothelial cells of capillaries (Fig. 4I *vs.* M, blue

arrowheads) though this colocalization does not provide information about whether the two types of cells had established proper communication. In conclusion, excess RA influenced the recruitment, stabilization and differentiation of PDGFRB-positive VSMC progenitors, and this effect was most apparent in the case of the large subepicardial veins of *Dhrs3*$^{-/-}$ embryos.

RA deficiency leads to defective formation of the myocardium and the coronary vessels

Previously we have described the establishment of a mid-gestational model of *in utero* RA deficiency by administration of Win 18, 446 (WIN), an irreversible inhibitor of the aldehyde dehydrogenase 1A (ALDH1A) family of enzymes, which convert retinaldehyde to RA (Chen et al., 2018). WIN, having been briefly investigated as a potential male contraceptive (Heller et al., 1961), was shown to be a potent inducer of congenital heart defects including coronary defects, yet, the cause for such defects remains poorly understood (Oster et al., 1974; Kilburn et al., 1982; Binder, 1985; Tasaka et al., 1991; Ito et al., 1992; Okishima et al., 1992; Kuribayashi and Roberts, 1993; Jackson et al., 1995; Nishijima et al., 2000; Okamoto et al., 2004; Fujino et al., 2005; Kise et al., 2005; Hanato et al., 2011). We found that administration of WIN between E9.5 and E13.5 dramatically reduced the amount of RA and alters RA-signaling in developing mouse embryos and their hearts (Wang et al., 2018). Importantly, we also discovered that administration of WIN affects the reorganization of the epicardial cytoskeleton and the migration of EPDCs into the myocardium (Wang et al., 2018).

In this study, we also observed that WIN-treated embryos of C57/BL6 mice showed signs of edema possibly resulting from cardiac insufficiency (Fig. 6A *vs.* B). Despite apparently normal chamber formation, we noticed a 50% thinner myocardium compact zone in WIN-treated embryos when compared to the vehicle control-treated group (Fig. 6C *vs.* D, via hematoxylin and eosin quantified in 6K). Inadequate formation of RA during mid-gestation also led to coronary defects. Whole-mount immunostaining of endothelial cells via PECAM1 indicated that the coronary vessels failed to fully expand to the ventricular apices in WIN-treated hearts, whereas the vessels developed and sprouted normally in the hearts of the vehicle control group, (Fig. 6E *vs.* F, *red dashed*-line marks the edge of expanding vasculature). Quantification of vessel coverage revealed a 20% reduction in the hearts of the WIN-treated group compared to controls (Fig. 6L). In addition, RA deficiency also altered the vascular hierarchy of the coronary plexus. At E14.5, vehicle-treated embryonic hearts displayed a well-organized coronary vessel network with several major vessels developing from the AVC coursing towards the apex and branching out to smaller vessels (Fig. 6E). In contrast, WIN-treated embryos showed evidence of defects in the formation and maturation of the vascular network marked by having few clearly distinguishable major branches (quantified in Fig. 6M) and a conspicuous absence of the septal artery (Fig. 6F, yellow arrow), a normally constant feature of the control-treated mice and C57/BL6 mice in general (Fernandez et al., 2008). Upon examining intramyocardial vessel morphology we found that WIN treatment led to formation of vessels of a smaller diameter on average (Fig. 6G *vs.* H, quantified in N). Consistent with the reduced vascular coverage observed through whole-mount PECAM1 staining, the myocardium near the apex of the E14.5 WIN-treated heart

was devoid of vessels and the density of intramyocardial vessels was reduced overall in WIN-treated hearts (Fig. 6I *vs.* J, density quantified in 6O).

We next investigated the effect of WIN-reduced RA-signaling on the recruitment of VSMC progenitors to the coronary vessels of E14.5 embryos. Endothelial cells and VSMC progenitors were visualized by double immunostaining of PECAM1 (green) and PDGFRB (red), respectively, at E14.5 in embryonic hearts (Fig. 7). Previously, we reported reduced migration of epicardial cells in response to WIN treatment in both *in vivo* and *in vitro* models (Wang et al., 2018). Consequently, there were fewer PDGFRB-positive cells in the myocardium surrounding the coronary vessels of WIN-treated embryos (Fig. 7B *vs.* F). However, the few PDGFRB-positive EPDCs that had infiltrated the myocardium in WIN-treated mice reached positions near or adjacent to endothelial tubes (Fig. 7E, G), which indicates that the initial recruitment of VSMC progenitors to the coronary vessels is not severely altered as a consequence of reduced RA-signaling in the WIN-treated group.

RA-signaling influences the epicardial transcriptome and proteome

Both fetal and postnatal epicardium secretes signaling molecules that stimulate the growth and repair of the heart (Olivey and Svensson; Zhou et al., 2011). RA-signaling can stimulate epicardial cells to produce trophic factors that enhance the proliferation of cardiomyocytes (Chen et al., 2002; Stuckmann et al., 2003; Merki et al., 2005; Brade et al., 2011; Shen et al., 2015).

To define the effects of altered RA-signaling on epicardial cell signaling we performed transcriptome and proteome profiling on a ventricular epicardial cell line, mouse embryonic epicardial cell line 1 (MEC1) (Li et al., 2011), treated for 48 hr with 10nM TTNPB, a stable RAR pan-agonist. We identified 6,931 genes being differentially regulated in MEC1 cells by TTNPB treatment compared to the vehicle control-treated group (Wang et al., 2018), and 737 proteins whose expression level was altered in response to TTNPB (Fig. 8 inset). Of these we identified 311 genes whose expression was consistently altered at both the transcript and protein level (Fig. 8 and 9). Predictably, activation of RA- signaling in MEC1 epicardial cells led to upregulation of the expression of multiple known RA-modulated genes, including *Rarβ*, *Rbp1* and *Hoxa1* (Supplementary Table 2). TTNPB treatment also induced compensatory responses in RA metabolism by suppressing the expression of genes responsible for RA synthesis (*Raldh1*, *Raldh2*, and *Rdh10*) and inducing the expression of those whose products reduce RA formation or catalyze its degradation (*Cyp26a1*, *Cyp26b1* and *Dhrs3*).

Using the Ingenuity Pathway Analysis (IPA) package (Kramer et al., 2014), we analyzed the set of 311 genes considered differentially expressed at both the protein and transcript levels in MEC1 cells in response to TTNPB. Based on the number of genes and their role in each pathway we assigned an activation *Z*-score which correlates with the potential activation (positive) or downregulation of the specific pathway (negative) (Kramer et al., 2014) (Fig. 8 and 9). Of all genes differentially expressed at both the protein and transcript levels, the set of genes involved in signaling by Rho family GTPases achieved the highest *Z*-score (Fig. 8). This observation agrees with our findings that TTNPB influences the cytoskeletal rearrangement of epicardial cells via the Rho pathway (Wang et al., 2018). Related processes

that involve regulation of actin-based motility by Rho, cardiac hypertrophic signaling, Rac and PAK-signaling were also upregulated. In contrast, the antagonistic Rho GDP dissociation inhibitor (GDI) signaling pathway was downregulated. These observations are consistent with an increase in cell migration and cytoskeletal remodeling of epicardial cells in the presence of RAR agonists. When we employed the IPA Upstream Regulator Analysis algorithm we identified several potential upstream regulators which would be predicted to cause similar expression changes in MEC1 as TTNPB. Specifically, we found that TTNPB treatment of MEC1 cells evokes similar gene expression changes as the activation of cytokine (interferon), growth factor (EGFR), and serum response factor (SRF) signaling (Supplementary Table 3).

Next, we focused solely on the MEC1 transcriptome data set for clues regarding the roles of epicardial RA in the secretion of cardiotrophic factors. Genes involved in several developmentally important growth factor- and hypoxia-signaling pathways were determined to be differentially regulated by activation of RAR via the treatment of TTNPB (Supplementary Table 2). Within the list of differentially expressed genes, we also found that RAR-agonist treatment of MEC1 cells induced the expression of known cardiotrophic factors such as *Fgf2* and *Fgf9* (Lavine et al., 2005), as well as mediators of FGF signaling (Supplementary Table 2). Analysis of the transcriptome data derived from TTNPB or control-treated MEC1 cells also revealed that HIF-1α and IGF-signaling was broadly attenuated by activation of RAR in epicardial cells. This was evident by the down-regulation of *Hif1α* as well as multiple known effectors of HIF-1α signaling, including *Vegfa*, *Tgfa* and *Hyou1* (Supplementary Table 2). The expression of several angiopoietin and angiopoietin-like proteins known to be hypoxia-responsive were also observed to be altered in response to TTNPB-treatment in MEC1 epicardial cells. In conclusion, analysis of the RNAseq data revealed that RA alters the gene expression profile of epicardial cells resulting in alterations in growth-promoting and angiogenic pathways. Collectively, our results suggest that besides its well understood roles in early cardiogenesis, RA-signaling also plays critical roles in regulating the growth of the myocardium and the formation and maturation of the coronary vasculature (Fig. 10).

DISCUSSION

Deficiency or excess RA can result in various cardiovascular malformations in developing embryos (Lammer et al., 1985; Niederreither et al., 2001; Ryckebusch et al., 2008; Sirbu et al., 2008). Due to the essential roles of RA during early embryogenesis, changes in early embryonic RA-signaling often result in embryonic lethality. As a result, the role of RA in heart development during late gestation is less well understood. The main source of cardiac RA during late gestation heart development is the epicardium (Moss et al., 1998; Niederreither et al., 2002; Perez-Pomares et al., 2002). Therefore, we sought out to investigate whether alteration in epicardial RA-signaling during late gestation heart development influences epicardial-related developmental events.

We report here that either excess or deficiency of RA can cause defects in growth of the myocardial compact zone and in the formation of the coronary vasculature (summarized in Figure 10). Using *Dhrs3*$^{-/-}$ embryos, a mouse model exhibiting mildly elevated embryonic

RA (Billings et al., 2013; Wang et al., 2018), we showed that excess RA caused defects in the formation of the coronary vascular plexus and abnormalities in coronary vessel morphology and branching. These delays are accompanied by the formation of ectopic endothelial nodules and large aberrant subepicardial veins devoid of mature VSMCs, as seen in the few *Dhrs3*$^{-/-}$ embryos which survived to late gestation. The cardiac defects and embryonic lethality observed in *Dhrs3*$^{-/-}$ embryos could be averted by reducing the maternal vitamin A intake of the dam, thus, demonstrating that the effects of *Dhrs3*-ablation on development were, indeed, the result of excess RA. In a second approach, starting at mid-gestation, we administered WIN to block RA synthesis. By doing so, we avoided the lethality and early cardiogenic defects resulting from RA deficiency previously observed in embryos treated with WIN during early gestation (Oster et al., 1974). WIN-treated embryonic hearts were properly chambered and had similar gross morphology when compared to the vehicle-treated group, yet, experienced a 60% reduction in the global levels of all-*trans*-RA and showed very restricted RA-signaling at E14.5 (Wang et al., 2018). Importantly, RA deficiency caused by WIN administration led to the formation of predominantly small-caliber vessels with few major arterial branches. Therefore, our results establish a critical role for RA in the formation, remodeling and maturation of the coronary vasculature.

RA-signaling is a shared component of the pathways that control the EMT, migration and differentiation of epicardial cells. We have shown that RA-signaling plays an important role in the PDGF-induced cytoskeletal reorganization of epicardial cells by activating Rho-signaling (Wang et al., 2018). Epicardial expression of the RA synthetic enzyme, RALDH2, is controlled by WT1 and defects in epicardial EMT caused by ablation of WT1 can be partially rescued by RA supplementation (Guadix et al., 2011; von Gise et al., 2011). RA-signaling also plays an important role in the subsequent differentiation of epicardial cells into VSMCs by repressing the differentiation of EPDCs into VSMCs via TCF21 (Azambuja et al., 2010; Braitsch et al., 2012). Epicardial EMT and EPDC differentiation is also controlled by Hippo-signaling (Singh et al., 2016; Xiao et al., 2018). We and others have shown that the retinaldehyde reductase *Dhrs3* counteracts the formation of RA, and is a direct target of the Hippo effectors, Yes-associated protein (YAP) - TEA domain transcription factor (TEAD) (Billings et al., 2013; Wang et al., 2018; Xiao et al., 2018). Unrestricted Yap/Taz activity as a result of ablation of the Hippo kinases, Lats 1/2, results in increased *Dhrs3* expression, and is associated with reduced fibroblast differentiation, and coronary vascular defects (Xiao et al., 2018). Crosstalk of Hippo and RA-signaling has also been invoked in the case of neural crest cells (Hindley et al., 2016). In conclusion, RA-signaling plays important roles in epicardial EMT and differentiation acting in conjunction with major signaling pathways that regulate epicardial development, and organ size and patterning.

Recruitment of mural cells in the form of VSMCs and pericytes is required for proper angiogenic remodeling and maturation of vessels (reviewed in (Gaengel et al., 2009)). Defects in the formation or recruitment of VSMCs or pericytes can often lead to coronary vascular defects and decreased ventricular vascular coverage (Hellstrom et al., 1999; Hellstrom et al., 2001; Mellgren et al., 2008; Smith et al., 2011; Trembley et al., 2015; Volz et al., 2015). Consequently, defects in VSMC/pericyte formation or recruitment observed in

the hearts of *Dhrs3*$^{-/-}$ or WIN-treated embryos could account for the compromised coronary vessel remodeling and maturation seen in these models, however, this possibility will require further studies. Of note, analysis of the proteome and transcriptome of TTNPB-treated epicardial cells revealed that SRF could be a potential upstream activator of epicardial RA-signaling (Supplementary Table 3). SRF is known to induce the differentiation of epicardial precursors into VSMCs via Rho (Lu et al., 2001), and, through interactions with the myocardin-related transcription factor (MRTF)-A and -B, SRF is important for epicardial cell migration, pericyte differentiation and coronary angiogenesis (Trembley et al., 2015). The influence of SRF or MRTF on RA-signaling during the recruitment of VSMCs and pericytes to the endothelia is a potentially important subject for future studies.

RA generated from cardiac (epicardial) and extra-cardiac sources influences the secretion of cardiotrophic factors by the epicardium. The ventricular myocardium grows during mid-gestation and is sensitive to altered levels of RA-signaling in the heart (Sucov et al., 1994; Merki et al., 2005; Lin et al., 2010). Notably, among differentially expressed proteins and genes in RAR agonist-treated epicardial MEC1 cells we identified FGF2, FGF9, thymosin β4, and follistatin-like 1 (FSTL1), all previously proposed to be involved in myocardial growth and coronary vascularization (Lavine et al., 2005; Pennisi and Mikawa, 2005; Smart et al., 2007; Vega-Hernandez et al., 2011; Wei et al., 2015). Importantly, RA had been previously shown to induce the expression of the epicardial mitogen FGF9 which controls myocardial proliferation (Lavine et al., 2005). The growth of the myocardium is also dependent on epicardial IGF2, whose expression was at first proposed to be controlled by epicardial RA (Chen et al., 2002; Stuckmann et al., 2003; Merki et al., 2005), and more recently shown to depend on RA-signaling in extra-cardiac (liver and placental) tissues signaling controlled at first by EPO and later by the placenta (Brade et al., 2011; Shen et al., 2015). We observed that in MEC1 epicardial cells, the expression of IGF2 was down-regulated in response to TTNPB treatment (Supplementary Table 2) consistent with the explanation that IGF2 secretion by the epicardium relies on signaling from RA produced by extra-cardiac sources. Since WIN-exposure and *Dhrs3*-deficiency affect RA signaling globally, we cannot exclude that altered RA signaling in extracardiac tissues may also indirectly contribute to the myocardial growth defects observed in these models. However, based on the effects observed in isolated epicardial explants and cell culture (Wang et al., 2018), it is evident that intrinsic epicardial RA signaling plays a non-redundant role in the formation, migration and differentiation of EPDCs.

Alterations in RA-signaling during late gestation heart development often translate into defects in both myocardial growth and the formation of the coronary vasculature (Fig. 10). For example, a hypoplastic ventricle and coronary vascular defects have been observed in mice with either an epicardial-ablation of RXR (Merki et al., 2005) or a deficiency in RALDH2 (Lin et al., 2010). Here, we show that embryos experiencing RA excess, or deficiency exhibited defects in formation of the primary coronary plexus and that their coronary vessels did not become invested with mature VSMCs. In the above-mentioned examples the coronary vascular defects were often accompanied by a hypoplastic myocardium and, in some cases, by other cardiac defects in outflow tract formation, chamber formation and septation (Sucov et al., 1994; Lin et al., 2010; Billings et al., 2013). In the current study, we observed that RA treatment of MEC1 epicardial cells caused a

reduction in the expression of factors involved in HIF1α-signaling and angiopoiesis. HIF1α-signaling in both the myocardium and epicardium is developmentally important for fetal growth, angiogenesis and the proper formation of the coronary vessels (Yue and Tomanek, 1999; Tomanek et al., 2003; Wikenheiser et al., 2006; Tao et al., 2013). However, since the growth of the compact zone of the myocardium is dependent upon the proper provision of oxygen and nutrients via the coronary vasculature, excessive hypoxia resulting from coronary defects may ultimately compromise its growth (Ream et al., 2008). The causal relationship among congenital coronary anomalies and other congenital cardiac defects is not currently understood. However, it is quite possible that they share common pathogenic mechanisms that influence each other through reciprocal interactions (Perez-Pomares et al., 2016).

In summary, these results contribute to our understanding of the importance of RA-signaling in cardiovascular development. While hepatic RA-supports erythropoiesis via EPO, and myocardial expansion via epicardial IGF2 (Makita et al., 2001; Brade et al., 2011; Shen et al., 2015), epicardial RA stimulates myocardial growth via FGF, and controls coronary vascular development to support the growth of the myocardium (Lavine et al., 2005; Merki et al., 2005; Azambuja et al., 2010; von Gise et al., 2011; Braitsch et al., 2012; Wang et al., 2018; Xiao et al., 2018). Through these concurrent actions embryonic RA coordinates the timing of definitive erythropoiesis, myocardial growth and vascularization of the heart and plays an integral role throughout the development of the heart, its vascular system, and hematopoiesis (Xavier-Neto et al., 2015; Canete et al., 2017).

EXPERIMENTAL PROCEDURES

Mice

Dhrs3$^{+/-}$, *RARE-LacZ* and *Dhrs3*$^{+/-}$; *RARE-LacZ* mice have been previously described (Billings et al., 2013). The *RARE-LacZ* mice carry a *LacZ* gene under the control of an RA-inducible promoter (Rossant et al., 1991) and are available at the Jackson Laboratories identified as strain *RARE-hsp68LacZ*, stock 008477. Unless otherwise noted, mice have been maintained on 2018 chow diet (Envigo) containing 15 IU vitamin A/gram and kept in rooms with controlled temperature and humidity with a 12 hr light-dark cycle. Studies of the effect of WIN were performed on C57/BL6 mice purchased from Taconic.

After mating female mice were checked for vaginal plugs in the morning and that noon is considered as embryonic day (E0.5). Caesarean sections were performed at designated embryonic stages to harvest pups or embryonic tissues. All animal protocols were approved by the Institutional Animal Care and Use Committee at the University of Kansas.

Generation of *Dhrs3*$^{-/-}$ mice in vitamin A-deficient dams

Dhrs3$^{+/-}$ parent mice were kept on a vitamin A sufficient diet (VAS) and their female *Dhrs3*$^{+/-}$ offspring were reared on a vitamin A deficient (VAD) diet from weaning. VAD-fed female *Dhrs3*$^{+/-}$ mice were bred overnight with male *Dhrs3*$^{+/-}$ mice to generate VAD-*Dhrs3*$^{-/-}$ embryos. Caesarean sections were performed at designated embryonic stages to harvest pups. In other studies, we continued the VAD diet of dams over successive

generations while mating to male *Dhrs3*$^{+/-}$ mice and genotyping for presence of living *Dhrs3*$^{-/-}$ mice. Both VAS and VAD diets are derived from AIN-93G growing rodent diet (Reeves, 1997). The VAS diet contained 4 IU of preformed vitamin A per gram of food (D13112B, Research Diets) whereas the VAD diet is deficient in both preformed vitamin A and provitamin A carotenoids (D13110GC, Research Diets).

Whole-mount PECAM1 and COUP TF II staining

Mouse embryonic hearts were isolated in PBS and fixed in 4% paraformaldehyde (PFA) at 4°C overnight. Hearts were dehydrated through a series of increasingly concentrated methanol/PBS into 100% methanol. Endogenous horseradish peroxidase activity in the heart was quenched by Dent's bleach (Methanol: DMSO: 30%H_2O_2=4:1:1) at room temperature for 4 hours and then the hearts were rehydrated through a decreasing methanol/PBS series into 100% PBS. Embryonic hearts were blocked in blocking buffer (5% non-fat milk/0.1% Tween 20/PBS) for 2 hours and then incubated with diluted primary antibody against platelet/endothelial cell adhesion molecule 1 (PECAM1) (1:500, Cat# 553370; BD-Pharmingen) for an hour at room temperature and subsequently overnight at 4°C. The specificity of antibodies employed has been validated by western blotting. After washing with PBS, a HRP-conjugated secondary antibody recognizing the species of the primary antibody was applied to samples and incubated for an hour. Detection of HRP was performed using the DAB Peroxidase substrate kit (Vector Laboratories, Cat# SK-4100) and the stained hearts were photographed and documented using a Leica DMS300 Dissection Microscope equipped with digital camera. *In situ* hybridization of chicken ovalbumin upstream promoter transcription factor (COUP-TF)-II in E9.5 embryonic hearts was performed as previously described (Bruneau et al., 2001). For each embryonic stage, at least 3 distinct mouse embryos of each genotype or treatment group were analyzed by whole-mount PECAM1 immunostaining.

Immunofluorescent staining

Immunofluorescent staining was carried out as previously reported (Billings et al., 2013). Embryos at various developmental stages were harvested in ice-cold PBS, fixed in 4% PFA overnight at 4°C, embedded in paraffin and transverse sectioned. Sample sections were deparaffinized and rehydrated at room temperature. Antigen retrieval methods specifically adapted in the case of different antigens were then applied: for CD31, sections were treated with 0.1mg/ml proteinase K for 5 minutes at room temperature; for PDGFRA/B and COUP-TF II, heat-mediated antigen retrieval was performed using pH6.0 trisodium citrate solution. In case of double-stained slides, embryonic tissues were fixed for 2 hours at 4°C and processed for frozen sectioning. Tissue sections were incubated with 3% H_2O_2 for 5 min to quench endogenous HRP activity, and were blocked with blocking buffer (5% normal goat serum/0.1% Tween 20/PBS) for an hour at room temperature, to prevent non-specific binding. Diluted primary antibody was subsequently added to slides and incubated at 4°C overnight. Primary antibodies employed are listed in Supplementary Table 1. After washing with 0.1% Tween 20/PBS solution, an Alexa Fluor-conjugated secondary antibody that recognizes the species of the primary antibody was applied. If signal amplification was needed, an HRP-conjugated secondary antibody was used together with the TSA Plus Fluorescein Evaluation Kit (PerkinElmer, Cat# NEL741E001KT) according to the

manufacturer's protocol. Nuclei were stained with 1 μM DAPI (Life Technologies) and sections were mounted with Vectashield mounting medium (Vector Laboratories, Cat# H-1000). Images were acquired either using a 20× air objective (0.3NA, Olympus Scientific Solutions Americas) on an inverted epifluorescent microscope (Olympus IX-81 with ZDC, Olympus Scientific Solutions Americas) with Hamamatsu Flash 4.0 v1 CMOS camera (Hamamatsu Corporation), or by a 40× oil objective (1.3NA, Olympus Scientific Solutions Americas) on an Olympus 3I spinning disk confocal microscope (Olympus IX-81, Olympus Scientific Solutions Americas) equipped with Andor Zyla 4.2 CMOS camera (Andor Technology Ltd). Images were representative of at least 5 images collected from each biological replicate. The intensity and contrast of each image were adjusted simultaneously and globally to accomplish a fair comparison between images.

Histology

Mouse embryos were isolated at E14.5 and fixed overnight in 4% paraformaldehyde at 4°C. Fixed embryos were embedded in paraffin and transverse sectioned at 7μm with a Leica RM2255 microtome. The slides were stained using hematoxylin and eosin reagents as previously described (Fischer et al., 2008). Staining results were documented using a Leica DMS300 Dissection Microscope equipped with digital camera.

LacZ staining

Dhrs3$^{+/-}$; *RARE-LacZ* mice were mated to produce *Dhrs3*$^{-/-}$; *RARE-LacZ* and *Dhrs3*$^{+/+}$; *RARE-LacZ* embryos which were isolated at various developmental stages and stained for LacZ activity as previously described (Billings et al., 2013). Samples in both experimental and control groups were processed simultaneously using identical protocols and incubation times and documented using a Leica DMS300 Dissection Microscope equipped with a digital camera.

Transcriptome analysis

MEC1 cells were treated with vehicle (DMSO) or 10nM TTNPB for 48 hours. Total RNA was isolated from 4 independent biological replicates per treatment using TRIzol reagent (Cat # 15596026, Thermo Fisher Scientific, Waltham MA) according to manufacturer's protocol and stored at −80°C. RNASeq was performed as described (Wang et al., 2018). The sequencing data is deposited at the NCBI Sequence Read Archive (SRA) as SRP132380.

Proteome analysis

Mouse MEC1 cells treated with 10 nM TTNPB, or DMSO-vehicle control for 48 hrs were lysed in 5 % sodium deoxycholate after washing in phosphate-buffered saline using three biological replicates for each treatment. Lysates were washed, reduced, alkylated and trypsinolyzed on filter based on previously described methods. (Wisniewski et al., 2009; Erde et al., 2014). Tryptic peptides were separated on a nanoACQUITY UPLC analytical column (CSH130 C18, 1.7 μm, 75 μm × 200 mm, Waters) over a 180-minute linear acetonitrile gradient (1–40%) with 0.1 % formic acid on a Waters nano-ACQUITY UPLC system, and analyzed on a coupled Thermo Scientific Orbitrap Fusion Tribrid mass spectrometer as previously described (Williamson et al., 2016). Full scans were acquired at a

resolution of 120,000, and precursors were selected for fragmentation by collision-induced dissociation (normalized collision energy at 35%) for a maximum 3-second cycle. Tandem mass spectra were searched against a UniProt mouse reference proteome using a Sequest HT algorithm as previously described (Eng et al., 2008) with a maximum precursor mass error tolerance of 10 ppm. Carbamidomethylation of cysteine and deamidation of asparagine and glutamine were treated as static and dynamic modifications, respectively. Resulting hits were validated at a maximum false discovery rate of 0.05 using a semi-supervised machine learning algorithm Percolator developed by Käll *et al.* (Kall et al., 2007). Protein abundance ratios between the TTNPB treated cells and the vehicle control were measured by comparing the MS1 peak volumes of peptide ions, whose identities were confirmed by MS2 sequencing as described above. Label-free quantifications were performed using an aligned AMRT (Accurate Mass and Retention Time) cluster quantification algorithm developed by Qi *et al.* (Qi et al., 2012). Of the 4,562 protein species detected, 3,543 were quantifiable. Differential expression analysis of the three TTNPB versus the three DMSO data sets revealed that 737 protein species were differentially expressed ($p<0.05$), of which 301 protein species had a fold change greater than 1.5, and 114 protein species had a fold change greater than 2. Pathway and upstream regulator analysis were performed using the Ingenuity Pathway Analysis package (QIAGEN Bioinformatics) as described (Kramer et al., 2014).

Statistical analysis

Data were represented means ± standard deviation and unpaired Student's *t*-test was utilized to evaluate statistical difference between groups.

Supplementary Material

Refer to Web version on PubMed Central for supplementary material.

Acknowledgments

Funding Information:

- NIH Grant Number: R01HD077260. Sponsor: NIH, Eunice Kennedy Shriver National Institute of Child Health and Human Development
- Fulbright U.S. Scholar Award- Brazil Scientific Mobility Program. Sponsors: Department of State, Bureau of Educational and Cultural Affairs and CAPES, the Brazilian Federal Agency for Support and Evaluation of Graduate Education,

We are grateful to Henry Sucov, University of Southern California, Los Angeles, CA, for his kind gift of the MEC1 cell line. This work was supported in part by the grant R01HD077260 from the National Institutes of Health (M.A.K., P.A.T., A.R.M.) and by a Fulbright U.S. Scholar Award funded by the U.S. Department of State's Bureau of Educational and Cultural Affairs, the Commission for Educational Exchange between the United States of America and Brazil and CAPES, the Brazilian Federal Agency for Support and Evaluation of Graduate Education (A.R.M.). Additional support was provided by startup funds to A.R.M. from the Northern Ontario School of Medicine. Conflicts of interest: none.

ABBREVIATIONS

AVC	atrioventricular canal
COUP-TF-II	chicken ovalbumin upstream promoter transcription factor
DHRS	dehydrogenase/reductase superfamily

EMT	epithelial-to-mesenchymal transition
EPO	erythropoietin
IGF	insulin-like growth factor 2
LacZ	beta-galactosidase
LC-MS/MS	liquid chromatography-tandem mass spectrometry
PDGF	platelet-derived growth factor
PDGFRA	platelet-derived growth factor receptor A
PDGFRB	platelet-derived growth factor receptor B
PECAM1	platelet/endothelial cell adhesion molecule 1
RA	all-*trans*-retinoic acid
RALDH	retinaldehyde dehydrogenase
RAR	retinoic acid receptor
RARE	retinoic acid response element
RhoA	Ras homolog gene family, member A
RXR	retinoid X receptor
SMAα	smooth muscle α-actin
SRF	serum response factor
TGFβ2	tumor-derived transforming growth factor-β2
VSMC	vascular smooth muscle cells
WIN	WIN18,446
WT1	Wilms-tumor 1

References

Ackermans MM, Zhou H, Carels CE, Wagener FA, Von den Hoff JW. Vitamin A and clefting: putative biological mechanisms. Nutr Rev. 2011; 69:613–624. [PubMed: 21967161]

Adams MK, Belyaeva OV, Wu L, Kedishvili NY. The retinaldehyde reductase activity of DHRS3 is reciprocally activated by retinol dehydrogenase 10 to control retinoid homeostasis. J Biol Chem. 2014; 289:14868–14880. [PubMed: 24733397]

Azambuja AP, Portillo-Sanchez V, Rodrigues MV, Omae SV, Schechtman D, Strauss BE, Costanzi-Strauss E, Krieger JE, Perez-Pomares JM, Xavier-Neto J. Retinoic acid and VEGF delay smooth muscle relative to endothelial differentiation to coordinate inner and outer coronary vessel wall morphogenesis. Circ Res. 2010; 107:204–216. [PubMed: 20522805]

Billings SE, Pierzchalski K, Butler Tjaden NE, Pang XY, Trainor PA, Kane MA, Moise AR. The retinaldehyde reductase DHRS3 is essential for preventing the formation of excess retinoic acid during embryonic development. FASEB J. 2013; 27:4877–4889. [PubMed: 24005908]

Binder M. The teratogenic effects of a bis(dichloroacetyl)diamine on hamster embryos. Aortic arch anomalies and the pathogenesis of the DiGeorge syndrome. Am J Pathol. 1985; 118:179–193. [PubMed: 3970137]

Brade T, Kumar S, Cunningham TJ, Chatzi C, Zhao X, Cavallero S, Li P, Sucov HM, Ruiz-Lozano P, Duester G. Retinoic acid stimulates myocardial expansion by induction of hepatic erythropoietin which activates epicardial Igf2. Development. 2011; 138:139–148. [PubMed: 21138976]

Braitsch CM, Combs MD, Quaggin SE, Yutzey KE. Pod1/Tcf21 is regulated by retinoic acid signaling and inhibits differentiation of epicardium-derived cells into smooth muscle in the developing heart. Dev Biol. 2012; 368:345–357. [PubMed: 22687751]

Bruneau BG, Bao ZZ, Fatkin D, Xavier-Neto J, Georgakopoulos D, Maguire CT, Berul CI, Kass DA, Kuroski-de Bold ML, de Bold AJ, Conner DA, Rosenthal N, Cepko CL, Seidman CE, Seidman JG. Cardiomyopathy in Irx4-deficient mice is preceded by abnormal ventricular gene expression. Mol Cell Biol. 2001; 21:1730–1736. [PubMed: 11238910]

Canete A, Cano E, Munoz-Chapuli R, Carmona R. Role of Vitamin A/Retinoic Acid in Regulation of Embryonic and Adult Hematopoiesis. Nutrients. 2017:9.

Chanda B, Ditadi A, Iscove NN, Keller G. Retinoic acid signaling is essential for embryonic hematopoietic stem cell development. Cell. 2013; 155:215–227. [PubMed: 24074870]

Chen T, Chang TC, Kang JO, Choudhary B, Makita T, Tran CM, Burch JB, Eid H, Sucov HM. Epicardial induction of fetal cardiomyocyte proliferation via a retinoic acid-inducible trophic factor. Dev Biol. 2002; 250:198–207. [PubMed: 12297106]

Chen Y, Zhu JY, Hong KH, Mikles DC, Georg GI, Goldstein AS, Amory JK, Schonbrunn E. Structural Basis of ALDH1A2 Inhibition by Irreversible and Reversible Small Molecule Inhibitors. ACS Chem Biol. 2018

Clagett-Dame M, Knutson D. Vitamin A in reproduction and development. Nutrients. 2011; 3:385–428. [PubMed: 22254103]

Collins MD, Mao GE. Teratology of retinoids. Annu Rev Pharmacol Toxicol. 1999; 39:399–430. [PubMed: 10331090]

Cunningham TJ, Duester G. Mechanisms of retinoic acid signalling and its roles in organ and limb development. Nat Rev Mol Cell Biol. 2015; 16:110–123. [PubMed: 25560970]

Eng JK, Fischer B, Grossmann J, Maccoss MJ. A fast SEQUEST cross correlation algorithm. J Proteome Res. 2008; 7:4598–4602. [PubMed: 18774840]

Erde J, Loo RR, Loo JA. Enhanced FASP (eFASP) to increase proteome coverage and sample recovery for quantitative proteomic experiments. J Proteome Res. 2014; 13:1885–1895. [PubMed: 24552128]

Feng L, Hernandez RE, Waxman JS, Yelon D, Moens CB. Dhrs3a regulates retinoic acid biosynthesis through a feedback inhibition mechanism. Dev Biol. 2010; 338:1–14. [PubMed: 19874812]

Fernandez B, Duran AC, Fernandez MC, Fernandez-Gallego T, Icardo JM, Sans-Coma V. The coronary arteries of the C57BL/6 mouse strains: implications for comparison with mutant models. J Anat. 2008; 212:12–18. [PubMed: 18067545]

Fischer AH, Jacobson KA, Rose J, Zeller R. Hematoxylin and eosin staining of tissue and cell sections. CSH Protoc. 2008; 2008 pdb prot4986.

Frenz DA, Liu W, Cvekl A, Xie Q, Wassef L, Quadro L, Niederreither K, Maconochie M, Shanske A. Retinoid signaling in inner ear development: A “Goldilocks” phenomenon. Am J Med Genet A. 2010; 152A:2947–2961. [PubMed: 21108385]

Fujino H, Nakagawa M, Nishijima S, Okamoto N, Hanato T, Watanabe N, Shirai T, Kamiya H, Takeuchi Y. Morphological differences in cardiovascular anomalies induced by bis-diamine between Sprague-Dawley and Wistar rats. Congenit Anom (Kyoto). 2005; 45:52–58. [PubMed: 15904432]

Gaengel K, Genove G, Armulik A, Betsholtz C. Endothelial-mural cell signaling in vascular development and angiogenesis. Arterioscler Thromb Vasc Biol. 2009; 29:630–638. [PubMed: 19164813]

Guadix JA, Ruiz-Villalba A, Lettice L, Velecela V, Munoz-Chapuli R, Hastie ND, Perez-Pomares JM, Martinez-Estrada OM. Wt1 controls retinoic acid signalling in embryonic epicardium through transcriptional activation of Raldh2. Development. 2011; 138:1093–1097. [PubMed: 21343363]

Haeseleer F, Huang J, Lebioda L, Saari JC, Palczewski K. Molecular characterization of a novel short-chain dehydrogenase/reductase that reduces all-trans-retinal. J Biol Chem. 1998; 273:21790–21799. [PubMed: 9705317]

Hanato T, Nakagawa M, Okamoto N, Nishijima S, Fujino H, Shimada M, Takeuchi Y, Imanaka-Yoshida K. Developmental defects of coronary vasculature in rat embryos administered bis-diamine. Birth Defects Res B Dev Reprod Toxicol. 2011; 92:10–16. [PubMed: 21312320]

Heller CG, Moore DJ, Paulsen CA. Suppression of spermatogenesis and chronic toxicity in men by a new series of bis(dichloroacetyl) diamines. Toxicol Appl Pharmacol. 1961; 3:1–11. [PubMed: 13713106]

Hellstrom M, Gerhardt H, Kalen M, Li X, Eriksson U, Wolburg H, Betsholtz C. Lack of pericytes leads to endothelial hyperplasia and abnormal vascular morphogenesis. J Cell Biol. 2001; 153:543–553. [PubMed: 11331305]

Hellstrom M, Kalen M, Lindahl P, Abramsson A, Betsholtz C. Role of PDGF-B and PDGFR-beta in recruitment of vascular smooth muscle cells and pericytes during embryonic blood vessel formation in the mouse. Development. 1999; 126:3047–3055. [PubMed: 10375497]

Hindley CJ, Condurat AL, Menon V, Thomas R, Azmitia LM, Davis JA, Pruszak J. The Hippo pathway member YAP enhances human neural crest cell fate and migration. Sci Rep. 2016; 6:23208. [PubMed: 26980066]

Ito H, Iwasaki K, Ikeda T, Sakai H, Shimokawa I, Matsuo T. HNK-1 expression pattern in normal and bis-diamine induced malformed developing rat heart: three dimensional reconstruction analysis using computer graphics. Anat Embryol (Berl). 1992; 186:327–334. [PubMed: 1384394]

Jackson M, Connell MG, Smith A, Drury J, Anderson RH. Common arterial trunk and pulmonary atresia: close developmental cousins? results from a teratogen induced animal model. Cardiovasc Res. 1995; 30:992–1000. [PubMed: 8746216]

Kall L, Canterbury JD, Weston J, Noble WS, MacCoss MJ. Semi-supervised learning for peptide identification from shotgun proteomics datasets. Nat Methods. 2007; 4:923–925. [PubMed: 17952086]

Kam RK, Shi W, Chan SO, Chen Y, Xu G, Lau CB, Fung KP, Chan WY, Zhao H. Dhrs3 protein attenuates retinoic acid signaling and is required for early embryonic patterning. J Biol Chem. 2013; 288:31477–31487. [PubMed: 24045938]

Kilburn KH, Hess RA, Lesser M, Oster G. Perinatal death and respiratory apparatus dysgenesis due to a bis (dichloroacetyl) diamine. Teratology. 1982; 26:155–162. [PubMed: 6297112]

Kise K, Nakagawa M, Okamoto N, Hanato T, Watanabe N, Nishijima S, Fujino H, Takeuchi Y, Shiraishi I. Teratogenic effects of bis-diamine on the developing cardiac conduction system. Birth Defects Res A Clin Mol Teratol. 2005; 73:547–554. [PubMed: 15965974]

Kochhar DM. Limb development in mouse embryos. I. Analysis of teratogenic effects of retinoic acid. Teratology. 1973; 7:289–298.

Kolodzinska A, Heleniak A, Ratajska A. Retinoic acid-induced ventricular non-compacted cardiomyopathy in mice. Kardiol Pol. 2013; 71:447–452. [PubMed: 23788084]

Kramer A, Green J, Pollard J Jr, Tugendreich S. Causal analysis approaches in Ingenuity Pathway Analysis. Bioinformatics. 2014; 30:523–530. [PubMed: 24336805]

Kuribayashi T, Roberts WC. Tetralogy of Fallot, truncus arteriosus, abnormal myocardial architecture and anomalies of the aortic arch system induced by bis-diamine in rat fetuses. J Am Coll Cardiol. 1993; 21:768–776. [PubMed: 8436760]

Lai L, Bohnsack BL, Niederreither K, Hirschi KK. Retinoic acid regulates endothelial cell proliferation during vasculogenesis. Development. 2003; 130:6465–6474. [PubMed: 14627725]

Lajiness JD, Conway SJ. Origin, development, and differentiation of cardiac fibroblasts. J Mol Cell Cardiol. 2014; 70:2–8. [PubMed: 24231799]

Lammer EJ, Chen DT, Hoar RM, Agnish ND, Benke PJ, Braun JT, Curry CJ, Fernhoff PM, Grix AW Jr, Lott IT, et al. Retinoic acid embryopathy. N Engl J Med. 1985; 313:837–841. [PubMed: 3162101]

Lavine KJ, Yu K, White AC, Zhang X, Smith C, Partanen J, Ornitz DM. Endocardial and epicardial derived FGF signals regulate myocardial proliferation and differentiation in vivo. Dev Cell. 2005; 8:85–95. [PubMed: 15621532]

Lee LM, Leung CY, Tang WW, Choi HL, Leung YC, McCaffery PJ, Wang CC, Woolf AS, Shum AS. A paradoxical teratogenic mechanism for retinoic acid. Proc Natl Acad Sci U S A. 2012; 109:13668–13673. [PubMed: 22869719]

Lee RY, Luo J, Evans RM, Giguere V, Sucov HM. Compartment-selective sensitivity of cardiovascular morphogenesis to combinations of retinoic acid receptor gene mutations. Circ Res. 1997; 80:757–764. [PubMed: 9168777]

Li P, Cavallero S, Gu Y, Chen TH, Hughes J, Hassan AB, Bruning JC, Pashmforoush M, Sucov HM. IGF signaling directs ventricular cardiomyocyte proliferation during embryonic heart development. Development. 2011; 138:1795–1805. [PubMed: 21429986]

Lin SC, Dolle P, Ryckebusch L, Noseda M, Zaffran S, Schneider MD, Niederreither K. Endogenous retinoic acid regulates cardiac progenitor differentiation. Proc Natl Acad Sci U S A. 2010; 107:9234–9239. [PubMed: 20439714]

Lu J, Landerholm TE, Wei JS, Dong XR, Wu SP, Liu X, Nagata K, Inagaki M, Majesky MW. Coronary smooth muscle differentiation from proepicardial cells requires rhoA-mediated actin reorganization and p160 rho-kinase activity. Dev Biol. 2001; 240:404–418. [PubMed: 11784072]

Makita T, Hernandez-Hoyos G, Chen TH, Wu H, Rothenberg EV, Sucov HM. A developmental transition in definitive erythropoiesis: erythropoietin expression is sequentially regulated by retinoic acid receptors and HNF4. Genes Dev. 2001; 15:889–901. [PubMed: 11297512]

Mellgren AM, Smith CL, Olsen GS, Eskiocak B, Zhou B, Kazi MN, Ruiz FR, Pu WT, Tallquist MD. Platelet-derived growth factor receptor beta signaling is required for efficient epicardial cell migration and development of two distinct coronary vascular smooth muscle cell populations. Circ Res. 2008; 103:1393–1401. [PubMed: 18948621]

Merki E, Zamora M, Raya A, Kawakami Y, Wang J, Zhang X, Burch J, Kubalak SW, Kaliman P, Izpisua Belmonte JC, Chien KR, Ruiz-Lozano P. Epicardial retinoid X receptor alpha is required for myocardial growth and coronary artery formation. Proc Natl Acad Sci U S A. 2005; 102:18455–18460. [PubMed: 16352730]

Moss JB, Xavier-Neto J, Shapiro MD, Nayeem SM, McCaffery P, Drager UC, Rosenthal N. Dynamic patterns of retinoic acid synthesis and response in the developing mammalian heart. Dev Biol. 1998; 199:55–71. [PubMed: 9676192]

Niederreither K, Fraulob V, Garnier JM, Chambon P, Dolle P. Differential expression of retinoic acid-synthesizing (RALDH) enzymes during fetal development and organ differentiation in the mouse. Mech Dev. 2002; 110:165–171. [PubMed: 11744377]

Niederreither K, Vermot J, Messaddeq N, Schuhbaur B, Chambon P, Dolle P. Embryonic retinoic acid synthesis is essential for heart morphogenesis in the mouse. Development. 2001; 128:1019–1031. [PubMed: 11245568]

Nishijima S, Nakagawa M, Fujino H, Hanato T, Okamoto N, Shimada M. Teratogenic effects of bis-diamine on early embryonic rat heart: an in vitro study. Teratology. 2000; 62:115–122. [PubMed: 10931509]

Okamoto N, Nakagawa M, Fujino H, Nishijima S, Hanato T, Narita T, Takeuchi Y, Imanaka-Yoshida K. Teratogenic effects of bis-diamine on the developing myocardium. Birth Defects Res A Clin Mol Teratol. 2004; 70:132–141. [PubMed: 15039927]

Okishima T, Takamura K, Matsuoka Y, Ohdo S, Hayakawa K. Cardiovascular anomalies in chick embryos produced by bis-diamine in dimethylsulfoxide. Teratology. 1992; 45:155–162. [PubMed: 1615425]

Olivey HE, Svensson EC. Epicardial-myocardial signaling directing coronary vasculogenesis. Circ Res. 2010; 106:818–832. [PubMed: 20299672]

Oster G, Salgo MP, Taleporos P. Embryocidal action of a bis(dichloroacetyl)-diamine: an oral abortifacient for rats. Am J Obstet Gynecol. 1974; 119:583–588. [PubMed: 4857790]

Paschaki M, Schneider C, Rhinn M, Thibault-Carpentier C, Dembele D, Niederreither K, Dolle P. Transcriptomic analysis of murine embryos lacking endogenous retinoic acid signaling. PLoS One. 2013; 8:e62274. [PubMed: 23638021]

Pennisi DJ, Mikawa T. Normal patterning of the coronary capillary plexus is dependent on the correct transmural gradient of FGF expression in the myocardium. Dev Biol. 2005; 279:378–390. [PubMed: 15733666]

Perez-Pomares JM, de la Pompa JL, Franco D, Henderson D, Ho SY, Houyel L, Kelly RG, Sedmera D, Sheppard M, Sperling S, Thiene G, van den Hoff M, Basso C. Congenital coronary artery anomalies: a bridge from embryology to anatomy and pathophysiology--a position statement of the development, anatomy, and pathology ESC Working Group. Cardiovasc Res. 2016; 109:204–216. [PubMed: 26811390]

Perez-Pomares JM, Phelps A, Sedmerova M, Carmona R, Gonzalez-Iriarte M, Munoz-Chapuli R, Wessels A. Experimental studies on the spatiotemporal expression of WT1 and RALDH2 in the embryonic avian heart: a model for the regulation of myocardial and valvuloseptal development by epicardially derived cells (EPDCs). Dev Biol. 2002; 247:307–326. [PubMed: 12086469]

Qi D, Brownridge P, Xia D, Mackay K, Gonzalez-Galarza FF, Kenyani J, Harman V, Beynon RJ, Jones AR. A software toolkit and interface for performing stable isotope labeling and top3 quantification using Progenesis LC-MS. OMICS. 2012; 16:489–495. [PubMed: 22888986]

Ream M, Ray AM, Chandra R, Chikaraishi DM. Early fetal hypoxia leads to growth restriction and myocardial thinning. Am J Physiol Regul Integr Comp Physiol. 2008; 295:R583–595. [PubMed: 18509101]

Reeves PG. Components of the AIN-93 diets as improvements in the AIN-76A diet. J Nutr. 1997; 127:838S–841S. [PubMed: 9164249]

Rossant J, Zirngibl R, Cado D, Shago M, Giguere V. Expression of a retinoic acid response element-hsplacZ transgene defines specific domains of transcriptional activity during mouse embryogenesis. Genes Dev. 1991; 5:1333–1344. [PubMed: 1907940]

Rothman KJ, Moore LL, Singer MR, Nguyen US, Mannino S, Milunsky A. Teratogenicity of high vitamin A intake. N Engl J Med. 1995; 333:1369–1373. [PubMed: 7477116]

Rubin LP, Ross AC, Stephensen CB, Bohn T, Tanumihardjo SA. Metabolic Effects of Inflammation on Vitamin A and Carotenoids in Humans and Animal Models. Adv Nutr. 2017; 8:197–212. [PubMed: 28298266]

Ryckebusch L, Wang Z, Bertrand N, Lin SC, Chi X, Schwartz R, Zaffran S, Niederreither K. Retinoic acid deficiency alters second heart field formation. Proc Natl Acad Sci U S A. 2008; 105:2913–2918. [PubMed: 18287057]

Rydeen A, Voisin N, D'Aniello E, Ravisankar P, Devignes CS, Waxman JS. Excessive feedback of Cyp26a1 promotes cell non-autonomous loss of retinoic acid signaling. Dev Biol. 2015; 405:47–55. [PubMed: 26116175]

Shannon SR, Moise AR, Trainor PA. New insights and changing paradigms in the regulation of vitamin A metabolism in development. Wiley Interdiscip Rev Dev Biol. 2017:6.

Sharma B, Chang A, Red-Horse K. Coronary Artery Development: Progenitor Cells and Differentiation Pathways. Annu Rev Physiol. 2017; 79:1–19. [PubMed: 27959616]

Shen H, Cavallero S, Estrada KD, Sandovici I, Kumar SR, Makita T, Lien CL, Constancia M, Sucov HM. Extracardiac control of embryonic cardiomyocyte proliferation and ventricular wall expansion. Cardiovasc Res. 2015; 105:271–278. [PubMed: 25560321]

Singh A, Ramesh S, Cibi DM, Yun LS, Li J, Li L, Manderfield LJ, Olson EN, Epstein JA, Singh MK. Hippo Signaling Mediators Yap and Taz Are Required in the Epicardium for Coronary Vasculature Development. Cell Rep. 2016; 15:1384–1393. [PubMed: 27160901]

Sirbu IO, Zhao X, Duester G. Retinoic acid controls heart anteroposterior patterning by down-regulating Isl1 through the Fgf8 pathway. Dev Dyn. 2008; 237:1627–1635. [PubMed: 18498088]

Smart N, Risebro CA, Melville AAD, Moses K, Schwartz RJ, Chien KR, Riley PR. Thymosin [bgr]4 induces adult epicardial progenitor mobilization and neovascularization. Nature. 2007; 445:177–182. [PubMed: 17108969]

Smith CL, Baek ST, Sung CY, Tallquist MD. Epicardial-derived cell epithelial-to-mesenchymal transition and fate specification require PDGF receptor signaling. Circ Res. 2011; 108:e15–26. [PubMed: 21512159]

Stefanovic S, Zaffran S. Mechanisms of retinoic acid signaling during cardiogenesis. Mech Dev. 2017; 143:9–19. [PubMed: 28007475]

Stuckmann I, Evans S, Lassar AB. Erythropoietin and retinoic acid, secreted from the epicardium, are required for cardiac myocyte proliferation. Dev Biol. 2003; 255:334–349. [PubMed: 12648494]

Sucov HM, Dyson E, Gumeringer CL, Price J, Chien KR, Evans RM. RXR alpha mutant mice establish a genetic basis for vitamin A signaling in heart morphogenesis. Genes Dev. 1994; 8:1007–1018. [PubMed: 7926783]

Tao J, Doughman Y, Yang K, Ramirez-Bergeron D, Watanabe M. Epicardial HIF signaling regulates vascular precursor cell invasion into the myocardium. Dev Biol. 2013; 376:136–149. [PubMed: 23384563]

Tasaka H, Takenaka H, Okamoto N, Onitsuka T, Koga Y, Hamada M. Abnormal development of cardiovascular systems in rat embryos treated with bisdiamine. Teratology. 1991; 43:191–200. [PubMed: 2014482]

Tian X, Hu T, Zhang H, He L, Huang X, Liu Q, Yu W, He L, Yang Z, Zhang Z, Zhong TP, Yang X, Yang Z, Yan Y, Baldini A, Sun Y, Lu J, Schwartz RJ, Evans SM, Gittenberger-de Groot AC, Red-Horse K, Zhou B. Subepicardial endothelial cells invade the embryonic ventricle wall to form coronary arteries. Cell Res. 2013; 23:1075–1090. [PubMed: 23797856]

Tomanek RJ, Lund DD, Yue X. Hypoxic induction of myocardial vascularization during development. Adv Exp Med Biol. 2003; 543:139–149. [PubMed: 14713119]

Trembley MA, Velasquez LS, de Mesy Bentley KL, Small EM. Myocardin-related transcription factors control the motility of epicardium-derived cells and the maturation of coronary vessels. Development. 2015; 142:21–30. [PubMed: 25516967]

Vega-Hernandez M, Kovacs A, De Langhe S, Ornitz DM. FGF10/FGFR2b signaling is essential for cardiac fibroblast development and growth of the myocardium. Development. 2011; 138:3331–3340. [PubMed: 21750042]

Vieux-Rochas M, Coen L, Sato T, Kurihara Y, Gitton Y, Barbieri O, Le Blay K, Merlo G, Ekker M, Kurihara H, Janvier P, Levi G. Molecular dynamics of retinoic acid-induced craniofacial malformations: implications for the origin of gnathostome jaws. PLoS One. 2007; 2:e510. [PubMed: 17551590]

Volz KS, Jacobs AH, Chen HI, Poduri A, McKay AS, Riordan DP, Kofler N, Kitajewski J, Weissman I, Red-Horse K. Pericytes are progenitors for coronary artery smooth muscle. Elife. 2015:4.

von Gise A, Zhou B, Honor LB, Ma Q, Petryk A, Pu WT. WT1 regulates epicardial epithelial to mesenchymal transition through beta-catenin and retinoic acid signaling pathways. Dev Biol. 2011; 356:421–431. [PubMed: 21663736]

Wang S, Yu J, Jones JW, Pierzchalski K, Kane MA, Trainor PA, Xavier-Neto J, Moise AR. Retinoic acid signaling promotes the cytoskeletal rearrangement of embryonic epicardial cells. FASEB J. 2018 fj201701038R.

Wei K, Serpooshan V, Hurtado C, Diez-Cunado M, Zhao M, Maruyama S, Zhu W, Fajardo G, Noseda M, Nakamura K, Tian X, Liu Q, Wang A, Matsuura Y, Bushway P, Cai W, Savchenko A, Mahmoudi M, Schneider MD, van den Hoff MJ, Butte MJ, Yang PC, Walsh K, Zhou B, Bernstein D, Mercola M, Ruiz-Lozano P. Epicardial FSTL1 reconstitution regenerates the adult mammalian heart. Nature. 2015; 525:479–485. [PubMed: 26375005]

Wikenheiser J, Doughman YQ, Fisher SA, Watanabe M. Differential levels of tissue hypoxia in the developing chicken heart. Dev Dyn. 2006; 235:115–123. [PubMed: 16028272]

Williamson JC, Edwards AV, Verano-Braga T, Schwammle V, Kjeldsen F, Jensen ON, Larsen MR. High-performance hybrid Orbitrap mass spectrometers for quantitative proteome analysis: Observations and implications. Proteomics. 2016; 16:907–914. [PubMed: 26791339]

Wisniewski JR, Zougman A, Nagaraj N, Mann M. Universal sample preparation method for proteome analysis. Nat Methods. 2009; 6:359–362. [PubMed: 19377485]

Wu SP, Dong XR, Regan JN, Su C, Majesky MW. Tbx18 regulates development of the epicardium and coronary vessels. Dev Biol. 2013; 383:307–320. [PubMed: 24016759]

Xavier-Neto J, Sousa Costa AM, Figueira AC, Caiaffa CD, Amaral FN, Peres LM, da Silva BS, Santos LN, Moise AR, Castillo HA. Signaling through retinoic acid receptors in cardiac development: Doing the right things at the right times. Biochim Biophys Acta. 2015; 1849:94–111. [PubMed: 25134739]

Xiao Y, Hill MC, Zhang M, Martin TJ, Morikawa Y, Wang S, Moise AR, Wythe JD, Martin JF. Hippo Signaling Plays an Essential Role in Cell State Transitions during Cardiac Fibroblast Development. Dev Cell. 2018; 45:153–169. e156. [PubMed: 29689192]

Yasui H, Nakazawa M, Morishima M, Ando M, Takao A, Aikawa E. Cardiac outflow tract septation process in the mouse model of transposition of the great arteries. Teratology. 1997; 55:353–363. [PubMed: 9294880]

Yue X, Tomanek RJ. Stimulation of coronary vasculogenesis/angiogenesis by hypoxia in cultured embryonic hearts. Dev Dyn. 1999; 216:28–36. [PubMed: 10474163]

Zhou B, Honor LB, He H, Ma Q, Oh JH, Butterfield C, Lin RZ, Melero-Martin JM, Dolmatova E, Duffy HS, Gise A, Zhou P, Hu YW, Wang G, Zhang B, Wang L, Hall JL, Moses MA, McGowan FX, Pu WT. Adult mouse epicardium modulates myocardial injury by secreting paracrine factors. J Clin Invest. 2011; 121:1894–1904. [PubMed: 21505261]

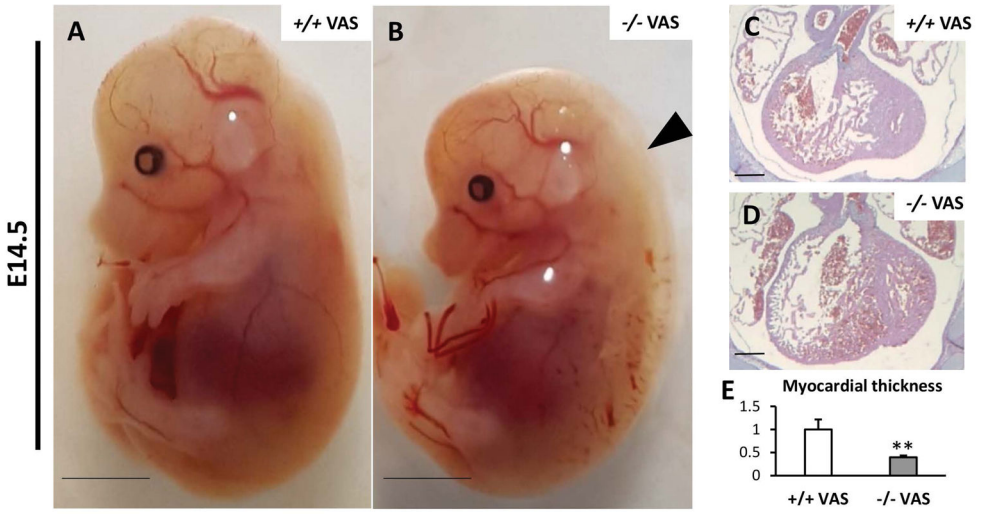

Figure 1.

Ablation of *Dhrs3* compromises myocardial growth. Genetic ablation of *Dhrs3* leads to subcutaneous edema at E14.5 (A–B) in *Dhrs3*$^{-/-}$ maintained on a vitamin A sufficient (VAS) diet. Examination of heart morphology at E14.5 revealed an evident reduction in myocardial thickness in ventricles of VAS-*Dhrs3*$^{-/-}$ (−/− VAS) embryos when compared to VAS-wild type (+/+ VAS) controls (**C**–**D,** via hematoxylin and eosin, quantified in **E**). Scale bars represent 2mm in A–B, 200μm in C–D. N=3 *Dhrs3*$^{-/-}$ *vs.* 3 wild type embryos. ** p<0.01 *vs.* VAS-WT

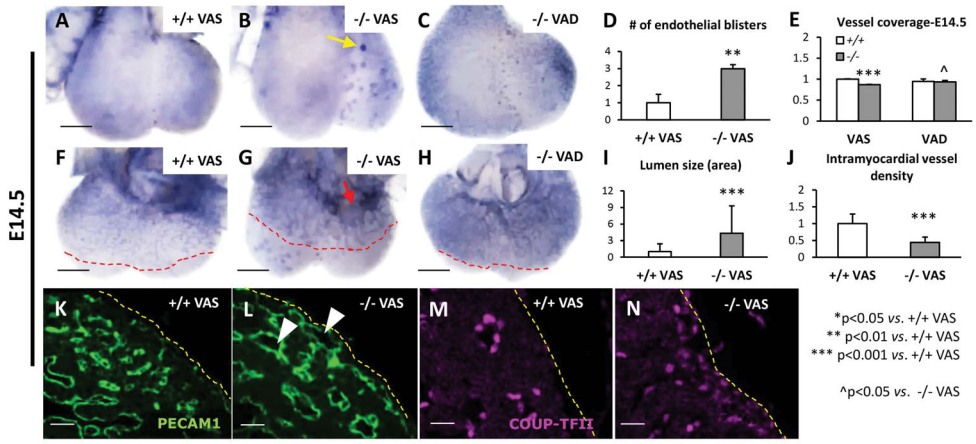

Figure 2.

Dhrs3 deficiency affects coronary development via excess RA. Whole-mount PECAM1 staining (*purple*) of endothelial cells revealed that E14.5 VAS-*Dhrs3*$^{-/-}$ (−/− VAS) embryos developed more numerous and larger ectopic endothelial nodules on the ventral side of the heart than VAS-wild type controls (+/+ VAS) (**A** *vs.* **B**, *yellow arrow*, numbers of nodules quantified in **D**). At E14.5 VAS-*Dhrs3*$^{-/-}$ embryos had a compromised vascular network morphology as well as reduced vascular expansion towards the apices compared to VAS-wild type controls (**F** *vs.* **G**, quantified in **E**; *red dashed lines* mark the apical edge of the plexus). Near the AVC of *Dhrs3*$^{-/-}$ hearts, the vessels fused to form a large diffuse endothelial trunk (**G**, *red arrow*). Feeding VAD diet to the dam restored the vascular coverage of E14.5 VAD-*Dhrs3*$^{-/-}$ embryos and decreased size and number of endothelial blisters compared to VAS-*Dhrs3*$^{-/-}$ embryos (**B** *vs.* **C**, **G** vs **H**, vascular coverage quantified in **E**). *Dhrs3*-deficiency resulted in enlargement of both intramyocardial and subepicardial coronary vessels (**K** *vs.* **L**, *white arrowheads*, lumen sizes are quantified in **I**), accumulation of superficially localized-veins (**M** *vs.* **N,** *yellow dashed line* marks the surface of the heart) and reduced intramyocardial vessel density (**J**) as observed via PECAM1 (in **K**, **L**, *green*) and COUP-TFII (in **M, N,** *violet*) immunostaining of sections of transversal sections. N=3 *Dhrs3*$^{-/-}$ *vs.* 3 wild type embryos. Scale bars represent, 400μm in A–C and F–H, 20μm in K–N. Error bars represent standard deviation. * p<0.05 *vs.* VAS-wild type; ** p<0.01 *vs.* VAS- wild type; *** P<0.001 *vs.* VAS- wild type; ^ p<0.05 *vs* VAS-*Dhrs3*$^{-/-}$.

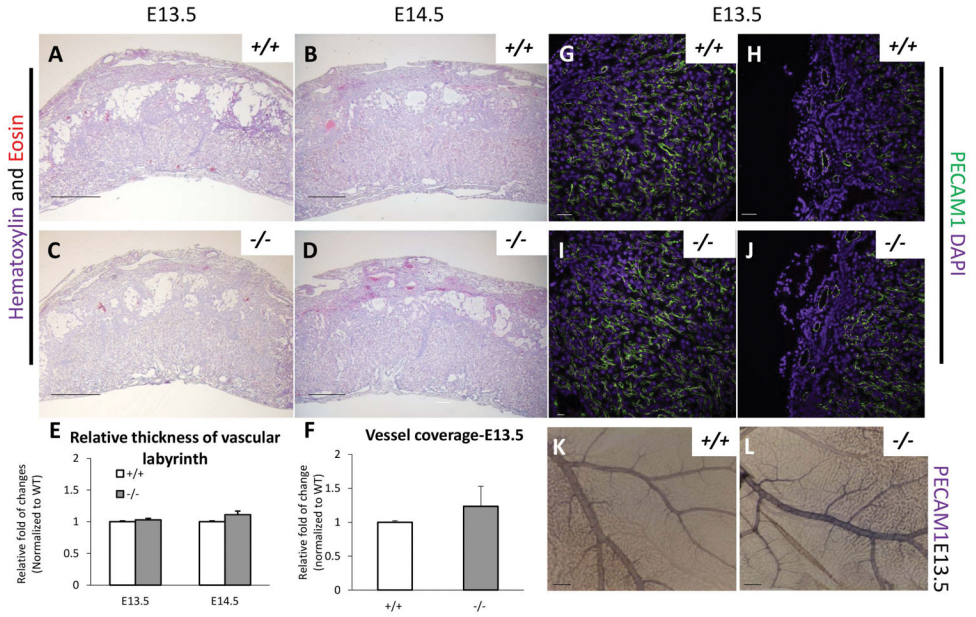

Figure 3.

The vascular development of the placenta is not affected by the absence of *Dhrs3*. Histology of the placenta of *Dhrs3*$^{-/-}$ and wildtype embryos at E13.5 (**A** *vs.* **C**) and E14.5 (**B** *vs.* **D**) as visualized via hematoxylin and eosin staining revealed it to be grossly normal. PECAM1 immunostaining of transversal sections of the placenta (**G**–**J**) suggested that ablation of *Dhrs3* does not significantly alter the thickness of vascular labyrinth layer (**E**) or the vascularization of the placenta (**F**). The number and branching pattern of the vessels in the yolk sac at E13.5 was found to be comparable between *Dhrs3*$^{-/-}$ and wildtype embryos. N=3 *Dhrs3*$^{-/-}$ *vs.* 3 wild type embryos for each developmental stage. Scale bars represent 50μm.

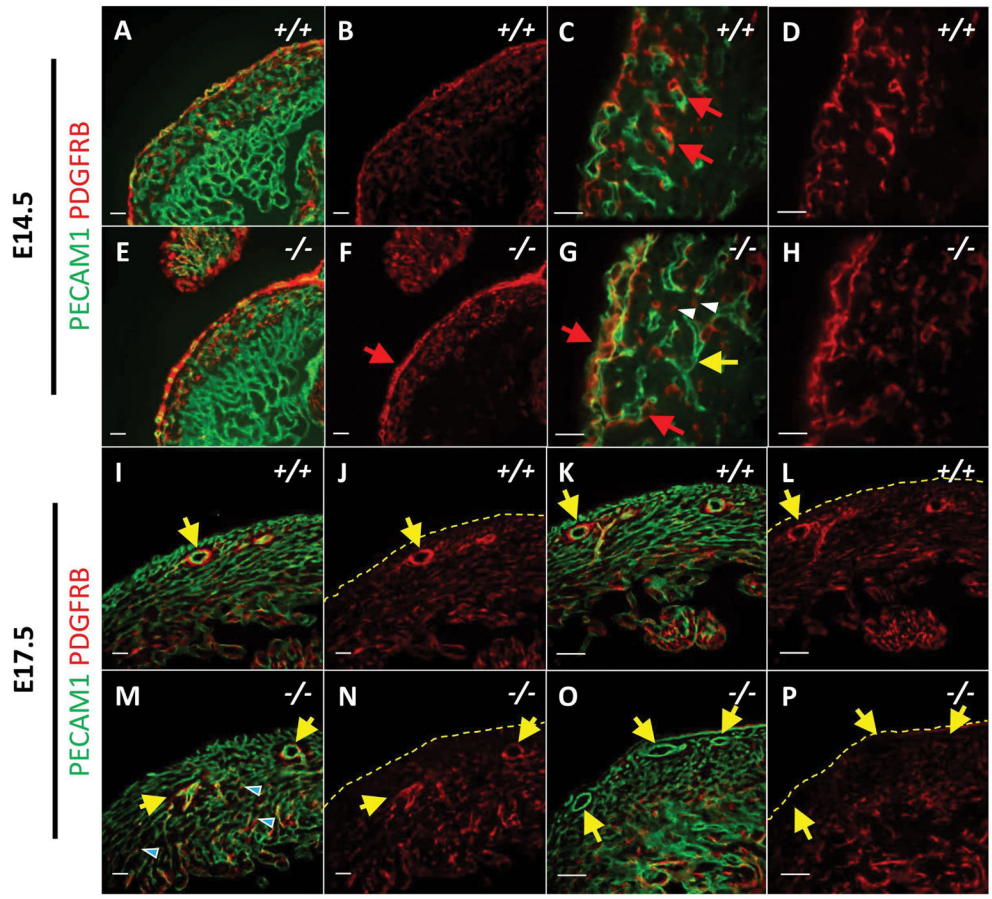

Figure 4.

RA excess due to *Dhrs3*-ablation affects the recruitment of PDGFRB-positive VMSC progenitor cells to endothelial tubes. At E14.5, PDGFRB-positive (*red*) cells were found to be in juxtaposition to both superficial and deep PECAM1-positive (*green*) endothelial tubules of wild type (+/+) embryos (**A**–**D**, *red arrow*) and near the superficially-localized vessels in *Dhrs3*$^{-/-}$ (−/−) embryos (**E–H**, *red arrows*). There were PDGFRB-positive cells that were not associated with endothelial cells (**G**, *white arrowheads*), as there were PECAM1-positive vessels that were not associated with PDGFRB-positive cells in *Dhrs3*$^{-/-}$ hearts (**G,** *yellow arrow*). At E17.5, large-caliber intramyocardial vessels in the wild type embryos were surrounded by a layer of PDGFRB-positive, VMSC progenitor cells (**I–L,** *yellow dashed line* marks the surface of the heart). In contrast, vessels of similar size in *Dhrs3*$^{-/-}$ embryos had a thin, sparse coverage of PDGFRB-positive cells (**M**–**N**, *yellow arrows*). Many of the abnormally enlarged superficial, subepicardial vessels were found to be devoid of coverage by VMSCs at E17.5 in in *Dhrs3*$^{-/-}$ hearts (**O–P**, *yellow arrows*). However, the smaller PECAM1-positive vessels in *Dhrs3*$^{-/-}$ hearts seemed to be associated with PDGFRB-positive cells (*blue arrowheads*). N=3 *Dhrs3*$^{-/-}$ *vs.* 3 wild type embryos in A–H, and N=3 *Dhrs3*$^{-/-}$ *vs.* 4 wild type embryos in I–P. Scale bars represent 50μm in A–B, E–F, I–J and M–N; 20μm in C–D, G–H, K–L and O–P.

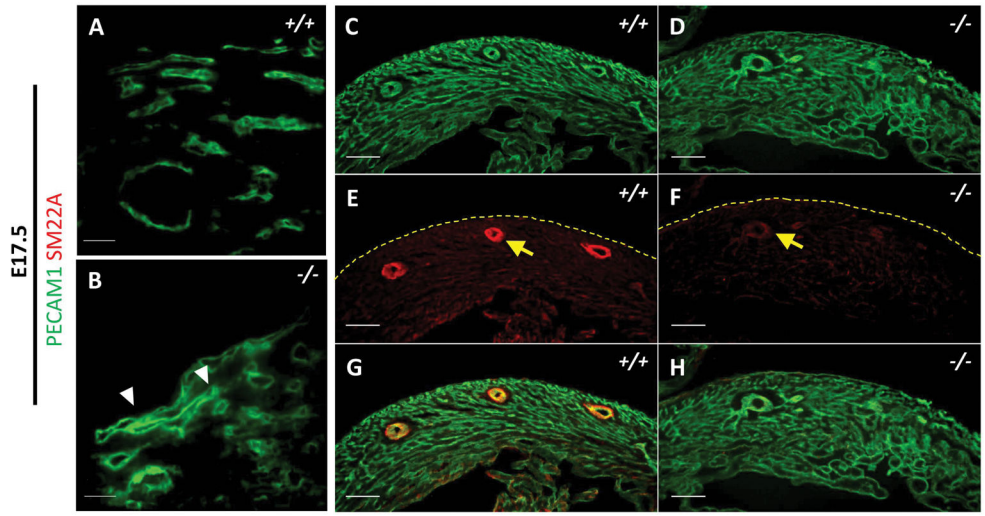

Figure 5.

RA excess due to *Dhrs3*-ablation affects the recruitment and differentiation of VSMCs. *Dhrs3*$^{-/-}$ hearts exhibited aberrantly enlarged PECAM1-positive vessels at E17.5 (**A** vs. **B**, marked by white arrow heads), when compared to wild type littermates. Double labeling of PECAM1 (*green*) and VSMC marker SM22A (*red*) in *Dhrs3*$^{-/-}$ (−/−) and wild type (+/+) embryonic hearts at E17.5 revealed a reduced expression of SM22A in the mural vascular cells of *Dhrs3*$^{-/-}$ embryos in contrast to the presence of SM22A-positive cells around vessels in the wild type hearts (**C** *vs.* **D**, *yellow arrow*). A *yellow dashed line* marks the surface of the heart. N=3 *Dhrs3*$^{-/-}$ *vs.* 4 wild type embryos. Scale bars represent 20μm in A–B, and 100μm in C–H.

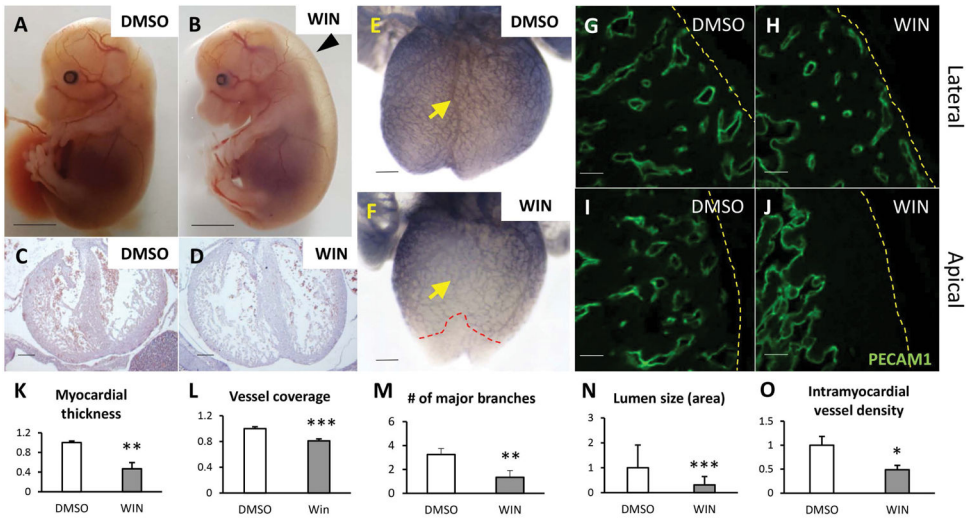

Figure 6.

RA deficiency compromises myocardial growth and coronary vessel formation. Embryos from dams treated with vehicle (**DMSO**) or WIN 18,446 (**WIN**) from E9.5 to E13.5 were isolated at E14.5. Embryos from the WIN-treated group showed evident subcutaneous edema (**A** *vs.* **B,** *arrow*), and significantly compromised growth of the ventricular myocardium as visualized by hematoxylin and eosin staining (**C** *vs.* **D**, quantified in **K**). Whole-mount PECAM1 immunostaining (**E, F**, *purple*) indicated that vehicle control-treated embryos develop a finely branched and a well-organized vascular network. In comparison, WIN treatment altered the number and localization of the major branches of vessels that sprout towards the apex of the heart (**E** *vs.* **F**, number of major branches was quantified in **M**) including the absence of the septal coronary artery (**E** *vs.* **F**, *yellow arrows*). WIN treatment resulted in a 20% reduction in vascular coverage of the ventricles when compared to the vehicle group (**E** *vs.* **F**, quantified in **L,** a *red dashed line* marks the apical edge of the vascular network on the dorsal side of ventricles) leading to avascular areas near the ventricular apices (**I** *vs.* **J**). Administration of WIN led to a reduction in the density and caliber of intramyocardial vessels (**G** *vs.* **H**, lumen sizes quantified in **N**, vessel density per area in the myocardium quantified in **O**) as revealed by PECAM1 (**G, I**, *green*) immunostaining of transversal sections (*yellow dashed line* marks the surface of the heart). N=4 WIN- *vs.* 4 DMSO-treated embryos. Scale bars represent 2mm in A–B, 200μm in C–F, 20μm in G–J.

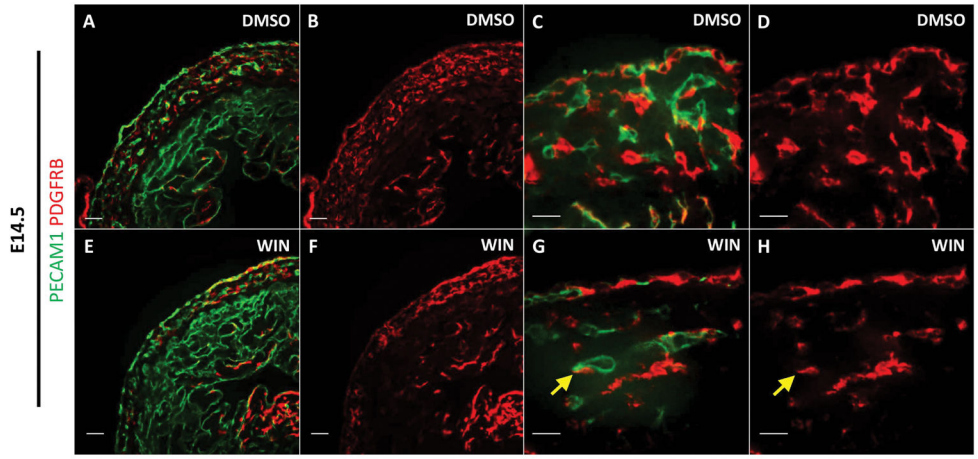

Figure 7.

RA deficiency alters the migration of epicardial-derived VSMC progenitor cells in WIN-treated embryonic hearts. Endothelial cells and VSMC progenitors were visualized by double immunostaining of PECAM1 (*green*) and PDGFRB (*red*) at E14.5 in embryonic hearts. When compared to vehicle control group, WIN-treated embryos have fewer coronary vessels in the myocardium, accompanied with decreased number of PDGFRB-positive VSMC progenitor cells in the myocardium (**B** *vs.* **F; D** *vs.* **H**). Though lower in number, the intramyocardial PDGFRB-positive cells in WIN-treated embryos were found to either surround or in proximity to vessels, similar to the vehicle control group. N=4 WIN- *vs.* 4 DMSO-treated embryos. Scale bars in A–B and E–F are 50μm and those in C–D and G–H are 20μm.

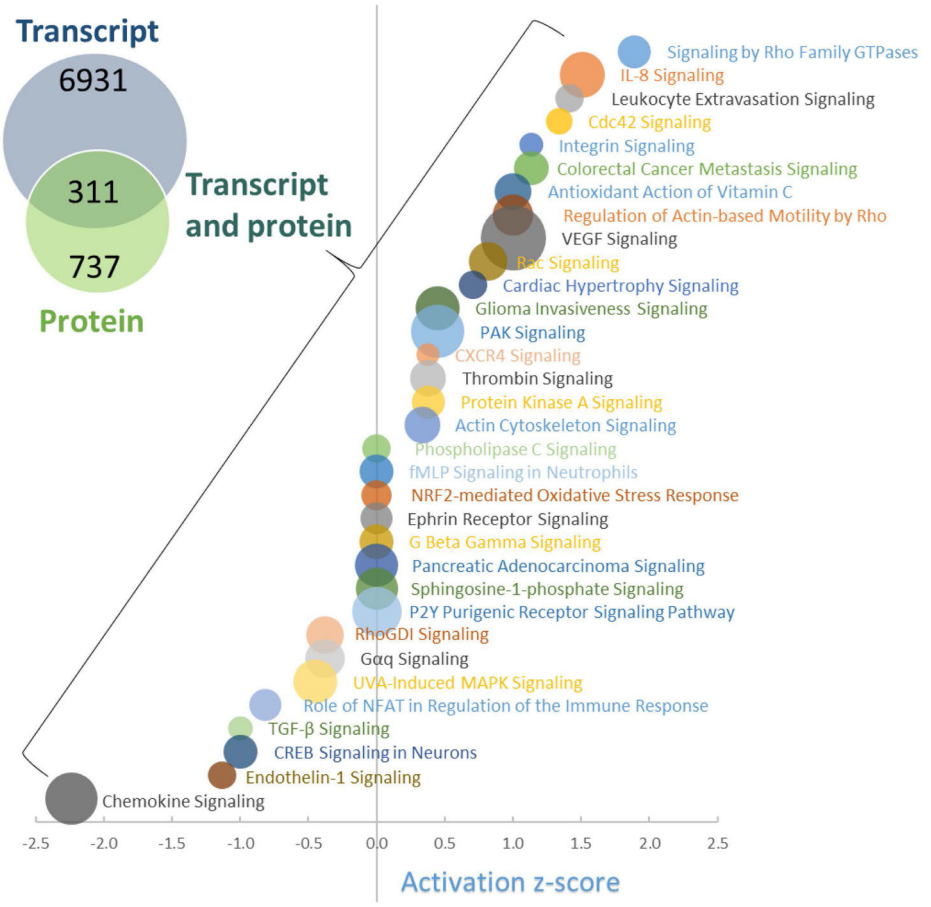

Figure 8.

Analysis of the genes differentially expressed in MEC1 cells treated with TTNPB. MEC1 cells were treated with 10nM TTNPB, or vehicle DMSO, for 48hrs following which the RNA was isolated and subjected to RNASeq as previously described (Wang et al., 2018). The protein isolated from MEC1 cells treated in the same manner was then used to analyze the proteome. The left inset Venn diagram shows the number of genes which are differentially expressed at transcript, or protein level, or at both. The 311 genes found to be differentially expressed based on both transcript and protein level were analyzed via Ingenuity Pathways whose categories are indicated in labels next to each bubble. The size of each bubble corresponds to the −log(p-value) and the x-axis displacement indicates the activation *Z*-score corresponding to potential upregulation or downregulation of the specific pathway. Analyses are based on the transcriptome and proteome profile of 4 WIN- *vs.* 4 DMSO-treated MEC1 cultures.

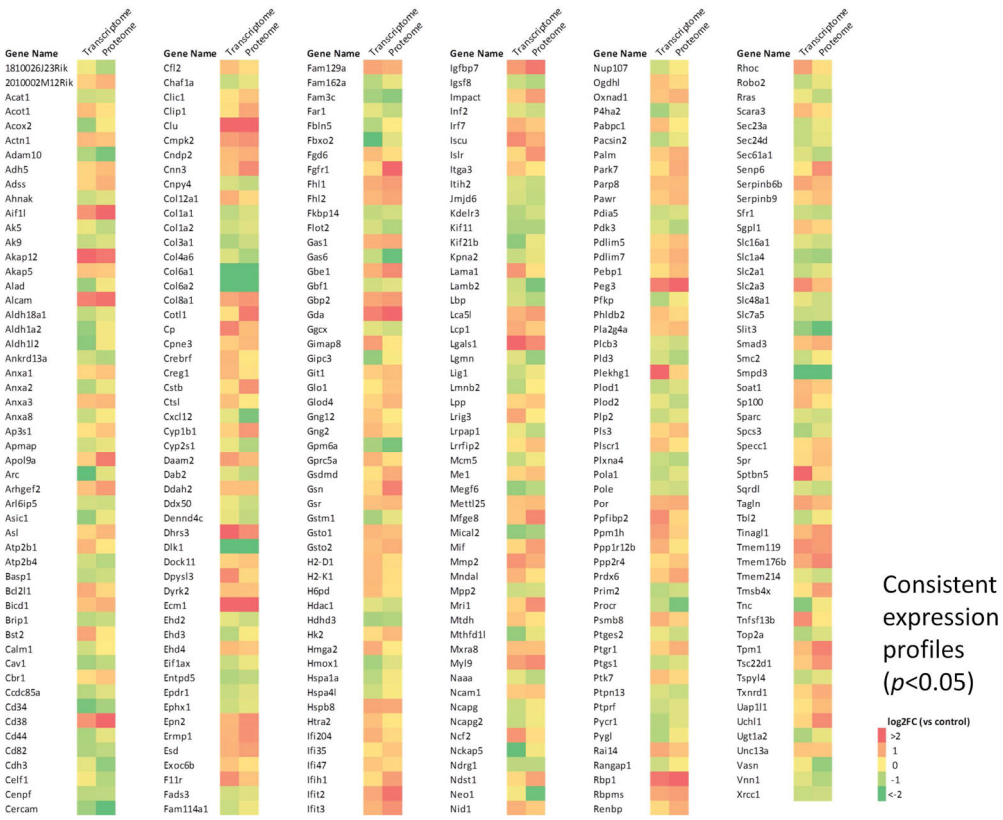

Figure 9.

Heatmap of 311 genes found be differentially expressed based on both transcriptome and proteome profiling of TTNPB-treated MEC1 cells. Fold changes of expression versus control are represented in a green (downregulated) to red (upregulated) gradient. Analyses are based on the transcriptome and proteome profile of 4 WIN- *vs.* 4 DMSO-treated MEC1 cultures.

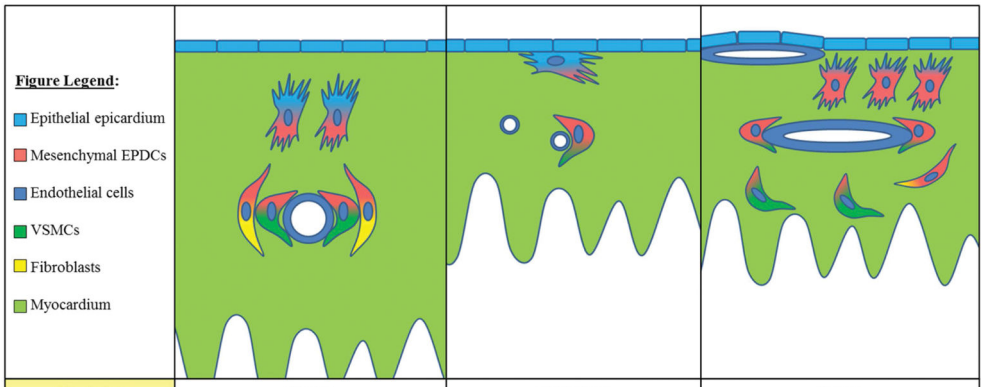

RA status	Normal	Deficiency	Excess
E14.5	Phenotype compared to normal heart	Thin myocardium	Thin myocardium
		Formation of microvessels at the expense of large vessels	Formation of large vessel at the expense of microvessels
		Low EMT	High EMT
		Lack of perivascular EPDCs	Excess EPDCs that are not associated with vessels
E17.5	Phenotype compared to normal heart	N/A	Lack of VSMCs

Figure 10.

Diagram summarizing our observations of the influence of altered RA-signaling on the formation of the coronary vasculature and the growth of the myocardial compact zone.